

Structural and biological study of synthesized anthraquinone series of compounds with sulfonamide feature

Pamita Awasthi, Manu Vatsal & Anjali Sharma

To cite this article: Pamita Awasthi, Manu Vatsal & Anjali Sharma (2018): Structural and biological study of synthesized anthraquinone series of compounds with sulfonamide feature, Journal of Biomolecular Structure and Dynamics, DOI: [10.1080/07391102.2018.1552198](https://doi.org/10.1080/07391102.2018.1552198)

To link to this article: <https://doi.org/10.1080/07391102.2018.1552198>



Accepted author version posted online: 29 Nov 2018.



Submit your article to this journal [↗](#)



Article views: 3



View Crossmark data [↗](#)

Structural and biological study of synthesized anthraquinone series of compounds with sulfonamide feature

^a Pamita Awasthi^{*}, Manu Vatsal^a, Anjali Sharma^a

^aDepartment of Chemistry, National Institute of Technology, Hamirpur, 177005, Himachal Pradesh, India.

Corresponding author address: Department of Chemistry, National Institute of Technology, Hamirpur, 177005, HP, India, Tel: 01972-254140

E-mail: pamitawasthi@gmail.com

Accepted Manuscript

ABSTRACT

1, 4 and 5, 8- positions as well as type of functionalities on these positions at anthraquinone-9, 10-dione are proposed to be significant for anticancer activity. Therefore, keeping this in to consideration, series of 1-substituted anthraquinone based compounds are designed, synthesized, characterized and biologically evaluated for anticancer activity. The structure of synthesized compounds are confirmed by spectroscopic analysis i.e. 1D (^1H and ^{13}C) NMR, ESI-MS studies, FT-IR tools. Synthesized 1-substituted anthraquinone compounds showed cytotoxic effect against MCF-7, PC-3 and Hep2C (Hela derivative) cell lines. All the compounds showed mild antibacterial property in comparison to standard antibiotic streptomycin against Gram +ve and –ve bacteria. They also exhibit mild antifungal activity. *In-vitro* ct-DNA binding studies of synthesized series using UV-Visible, Fluorescence tools indicates partial intercalative mode of binding. Electronic properties of synthesized analogues and Mitoxantrone are compared using HOMO-LUMO calculation. Low energy gap between HOMO-LUMO of 1-substituted anthraquinone compounds indicates the highly charged structure of the molecules in comparison to mitoxantrone and same is proposed to be responsible for comparable cytotoxic activities of the synthesized 1-substituted anthraquinone molecules. Docking interaction of synthesized 1-substituted anthraquinone compounds and i-motif sequence indicates intercalative mode of binding of compounds with telomeric junction.

Keywords: Anthraquinone; Sulfonamide; Mitoxantrone; HOMO-LUMO; Docking; Cytotoxicity; Antibacterial.

1. Introduction

Anticancer class of drugs includes large number of molecules which are divided on the basis of their mechanism of action like-alkylating agents, antimetabolites, anthracycline class of antibiotics, hormonal agents and signal transduction inhibitors (Beziane, Teerme, & Vanelle, 2005; Nor et al, 2013; Adachi et al, 2014; Krapcho, Getahun, Avery, Vargas, & Hacker, 1991; Guidi et al, 1994; Zuravka, Sosic, Gatto, & Gootlich, 2015). Anthracycline class of compounds are widely found in nature. The naturally occurring anthraquinones compounds carry a broad spectrum of bioactivities, such as antibacterial, antifungal, anticancer alongwith antioxidant activities (Zhang et al, 2011). The anthraquinone chromophore is an important structural feature

of the anthracycline class of antibiotics. Further anthracyclines are proved to be most effective for cancer treatment and use to treat cancers such as leukemia, lymphoma, breast uterine, ovarian, bladder and lung cancer. Some anthracycline class of drugs like daunorubicin, adriamycin, epirubicin and mitoxantrone are presently used in chemotherapy, however, major side effect associated with them is - cardiotoxicity. Mitoxantrone proposed to be less cardiotoxic than adriamycin and daunorubicin (Murdock, Child, Fabio, & Angier, 1979). Mitoxantrone has symmetrical structure consist of tricyclic planar anthraquinone chromophore with [(aminoethyl) amino]-ethanol side chain. Large number of analogues of mitoxantrone have been synthesized and biologically evaluated for their anticancer activity (Bailly, Routier, Bernier, & Waring, 1996; Sissi et al, 1999; Collier, & Neidle, 1988; Cheng-Zee, Robert, & Cheng, 1978; Cairns, Michalitsi, Jenkins, & Mackay, 2002; Routier, Bernier, Cateau, Riou, & Bailly, 1998; Horn et al, 2000). Further anthraquinone series of compound having amido linkage are reported in literature and interestingly some of these compounds showed good biological activity (Zagotto et al, 1997). Compounds with 1, 4 dihydrogen having longer side chains at 5, 8 position on anthraquinone ring showed better intercalative activity along with cytotoxicity at micro molar concentration. Further incorporation of amino acid in the side arms at 5,8 position on anthraquinone ring; followed the similar mechanism of interaction like that of Mitoxantrone (Zagotto, Sissi, Gatto, & Palumbo, 2004; Zagotto, Supino, Favini, Moro, & Palumbo, 2000; S-Aliabadi, Tabarzadi, & Zarghi, 2004). Analogues of 1-hydroxy derivative of anthraquinone showed significant anticancer activities against various cell lines. Further epoxidation of anthraquinone increases the cytotoxicity (Wei, Wu, Chung, Won, & Lin, 2000). Also modification of ketonic functionality of anthraquinone ring also reported in literature. Most of 9-substituted compounds are cytotoxic but lower than the Mitoxantrone (Konopa, 2001; Huang, Chiu, Lu, & Yuan, 2005).

Anthraquinone derivatives are proposed to be telomerase inhibitor and clinically proven to be the active site of drug interaction (Freccero et al, 2014; Chung et al, 2014; Balasubramanian, & Neidle, 2009). Telomeric activity is very high in cancer cells however low or nearly non-noticeable in normal cells as per literature review. Further -SO₂-NH- feature have been reported to bear anticancer activity. This feature has been proposed to show CDK2 inhibitory property and arrest cell cycle. Number of compounds with SO₂-NH- feature are synthesized and shown to be active against various cancer cell lines (Supuran, Briganti, Tilli, Chegwiddden, & Scozzafava, 2001; Fukuoka et al, 2001; Ella, Ghorab, Heiba, & Soliman, 2011). Further this feature has been

reported to show significant multifunctional activities (Alsughayer, Elassar, Mustafa, & Sagheer, 2011; Tan et al, 2011).

In present research paper we have incorporated 1-substituted sulfonamide functionality along with various amino acids i.e glycine, valine, phenylalanine and β -alanine in side chain on the anthraquinone chromophore. All molecules are synthesized in our laboratory under normal temperature pressure condition. The structure of all the molecules are confirmed by FT-IR, ESI-MS, PMR and ^{13}C -NMR spectrophotometric tools. All the 1- substituted synthesized compounds (S1-S8) are tested against MCF-7, PC-3 and Hela cancer cell lines. Likewise, compounds are also evaluated for their antibacterial, antifungal and antioxidant activity. Majority of 1-substituted compounds of the series are observed to be cytotoxic in comparison to Mitoxantrone. Detailed *in-vitro* binding study of 1-substituted synthesized molecules (S1-S8) has been carried out in comparison to Mitoxantrone using UV-visible and spectrofluoremetric tools. The study confirmed the partial intercalative mode of binding of 1-substituted synthesized molecules. Quantum chemical calculation indicates that synthesized 1-substituted molecules are highly charged in comparison to mitoxantrone which might suppose to facilitate DNA binding interactions at cellular level. Further, telomeric intercalation activity is confirmed by docking study on d (TC₅).

2. Material and methods

The compounds under investigation (S1-S8) were synthesized in our laboratory. The chemicals used for synthesis were purchased from Sigma-Aldrich with a stated purity of 97%. All solvents were distilled and dried, as per set methods and procedures, before use. Reactions were monitored by TLC performed on silica gel plates, the spots were located by iodine. Purity was checked in TLC with solvent system of benzene and methanol giving single spot. Melting points were uncorrected and measured in open capillary tubes on Digital Melting/Boiling point apparatus. The FT-IR spectrum of the compounds were collected in the frequency region of 4000-500 cm^{-1} using KBr pellet recorded on PERKIN ELMER spectrophotometer. The spectrum was recorded at room temperature, with a scanning speed of 8 $\text{cm}^{-1} \text{min}^{-1}$ with the spectral resolution of 8 cm^{-1} . ^1H NMR spectra were recorded in CDCl_3 and DMSO on a BRUKER AVANCE II 400 NMR spectrometer. Chemical shifts are given in ppm at 294.7 K. Mass spectral studies are carried out on ESI-MS instrument of Waters Micromass Q-ToF Micro; equipped with electrospray ionization (ESI) and atmospheric pressure chemical ionization (APCI) sources having mass range of 4000 amu in quadrupole and 20000 amu in ToF.

2.1. General procedure for the synthesis of (S1-S8) compounds

A mixture of benzene sulfonyl chloride (6.35ml, 0.05mol), different amino acids (0.05 mol) and NaOH sol (1N, 200ml) was stirred together at 45-50 °C for 4 hours. A clear solution was obtained and cooled to 5 °C and treated with conc. HCl to make it slightly acidic (pH-6.5). Benzene sulfonyl amino acid (**A**) was separated out as white crystals. Further benzene sulfonyl amino acids was stirred for 20 min. with the freshly prepared thionyl chloride (5.0g) and then refluxed for 3 hours to give acid chloride of benzene sulfonyl amino acid. Benzene sulfonyl amino acid chloride (0.003M) and 1-amino anthraquinone (0.004M) was then taken in dry benzene (1N), stirred together at 35-40 °C for 6-8 hours. It was then poured into ice- water mixture and extracted with chloroform. The extract was washed with excess of water. The solvent was then removed to leave a residue which was recrystallized from diethyl ether to give final product (**B**). The purity and reaction progress of the compound was checked by TLC (Vatsal, Devi, & Awasthi, 2018). The procedure is same for p-toluenesulfonyl amino acids. [Supplementary Fig. I (1a) and characterization (1b)].

2.2. Cytotoxicity assay

2.2.1. *In vitro* cytotoxicity analysis: [3-(4, 5-dimethylthiazol-2-yl)-2, 5-diphenyl tetrazolium bromide] (MTT) - based cytotoxicity assay against Hep2C.

The cytotoxic effects of synthesized compounds were carried out against Hep 2C Heal derivative (human cervix carcinoma) cell lines which were determined using MTT and compared with control. The cells were cultured in Dulbecco's Modified Eagle's Medium (DMEM) supplemented with 10% fetal calf serum, penicillin (100 units/ml) and streptomycin (100µg/ml) in a 5% CO₂-humidified atmosphere incubator. The cells were plated in a 96-well plate and treated with different concentrations of the compounds for 12 h in a CO₂ incubator (37°C, 5% CO₂ and 90% relative humidity). The cytotoxicity was measured by adding 20µl of freshly prepared MTT solution (5 mg/mL in PBS, sterile filtered) to each well. Culture plates were gently stirred at 150rpm for 5 min, to thoroughly mix the MTT into the media and incubated for another 3 h in dark at 37°C to allow metabolization of MTT. The purple formazan crystals were resuspended by adding 5mg/ml in methanol to each well. The absorbance was read at 570 nm in a spectrophotometer. The cell death was calculated as follows:

Cell death = 100 - [(test absorbance/control absorbance) × 100].

2.2.2 SRB (Sulforhodamine B) assay against MCF-7 (Human breast cancer cell line) and PC-3 (Human prostate cancer cell line).

Cells were inoculated into 96 well microtiter plates in 100 μ L. After cell inoculation, and before addition of experimental drugs plates were incubated at 37°C, 5% CO₂, 95 % air and 100 % relative humidity for 24 h. Experimental drugs were dissolved in dimethyl sulfoxide at 100mg/ml and diluted upto 1mg/ml using water. At the time of drug addition, an aliquot of frozen concentrate (1mg/ml) was thawed and diluted to 100 μ g/ml, 200 μ g/ml, 400 μ g/ml and 800 μ g/ml with complete medium containing test article. Aliquots of 10 μ l of these different drug dilutions were added to the appropriate microtiter wells already containing 90 μ l of medium, resulting in the required final drug concentrations i.e. 10 μ g/ml, 20 μ g/ml, 40 μ g/ml, 80 μ g/ml.

Further, plates were incubated under standard conditions for 48 hours. Cells were fixed *in situ* by the gentle addition of 50 μ l of cold 30 % (w/v) TCA (final concentration, 10 % TCA) and incubated for 60 minutes at 4°C. The supernatant was discarded and plates were washed five times with tap water and air dried. Sulforhodamine B (SRB) solution (50 μ l) at 0.4 % (w/v) in 1 % acetic acid was added to each of the wells followed by 20 minutes incubation at room temperature. Residual dye was removed by washing five times with 1 % acetic acid. The plates were air dried and stain was eluted with 10 mM trizma base. Absorbance was checked at a wavelength of 540 nm (SRB) with 690 nm reference (Mitoxantrone) wavelength. Percent growth was calculated for test wells relative to control wells. Percentage growth inhibition was calculated as: $[\text{Ti/C}] \times 100 \%$ (Vanicha Vichai & Kanyawim Kirtikara, 2006; Skehn et al, 1990).

2.2.3. Cell cycle analysis

Cell culture was trypsinized, and washed with phosphate buffered saline (PBS) and incubated at a density of 5×10^5 cells/well with 5 mL of complete medium in 6 well plate. Cells were grown in Dulbecco's Modified Eagle Medium (DMEM) supplemented with 10% fetal bovine serum and 1% antibiotic-antimycotic. Test samples dissolved in DMSO ([Dimethyl sulfoxide](#)) to make 10 mg/mL stock solution. Finally working concentration made by farther dilution of stock solution in complete medium and several dilutions of the test compounds in 1 mL of complete medium were added. Alone cells (without treatment) used as control. The plates were then incubated at 37°C for 12 to 24 hours in 5% CO₂ incubator. After Incubation period, both adherent and floating cells were harvested and centrifuged at 200 g for 5 min. Pellet were washed with phosphate buffer saline and again centrifuged at 200g for 5 min. After that, cell pellets were resuspended in

70% EtOH and fixed for 2h at 4 °C. Fixed cells were washed with PBS (14 mL) and centrifuged at 200g for 5 min. Cell pellets were resuspended in propidium iodide solution (50µg/mL in 0.1 % sodium citrate, 0.1 % Triton-X 100 and 20µg/ml RNAses A) for 30 min in dark. Samples were processed using an Amis flow cytometer. The distribution of cells in each phase of the cell cycle was calculated using IDEA software.

2.3. Preparation of solution for antibacterial and antifungal study

All the chemicals and solvents used in the present work were of analytical grade. A phosphate-buffer saline (PBS) was used as a diluents and prepared by dissolving 1.5mM disodium hydrogen phosphate, 0.5mM sodium phosphate, 10mM NaCl and 0.25mM EDTA at pH=7.1 using double distilled water. The Mueller-Hinton agar growth medium was nutrient broth for antibacterial assay and Potato dextrose agar for antifungal study. Streptomycin was used as an internal standard for Minimum inhibitory concentration in antibacterial assay. 200µl concentration range of streptomycin was prepared using PBS as an internal standard. The addition of 2µL microbes grown in nutrient broth and 2µL of solutions of varying concentrations of each compound dissolved in methanol to 96 microtiter plates. Six bacterial species, 3 gram-positive (*Salmonella. aureus*, *Salmonella epidermidis*, and *Salmonella. citreus*) and 3 gram negative (*Escherichia. coli*, *Klebscilla. pneumonia* and *Shigella. flexneri*) were used as target organisms in antibacterial assay and two fungi *Candida albicans* and *Mucor sps.* for antifungal activities. The plates were incubated and autoclaved.

2.3.1. Antibacterial activity assay

The nutrient agar and nutrient broth medium was prepared and then it was autoclaved. The agar medium poured in to the petriplates in a laminar flow and the media was left as it is overnight. The bacterial strains were spread over the media and left this for half an hour. The media containing the bacterial strains was punched with the help of the sterilized puncher. The compounds was dissolved in methanol were put inside the punched holes. The petri plates were left overnight in BOD incubator. The plates were incubated for 24 hours at 37°C then diameter of zone of inhibition was measured to know the antibacterial activity of the samples. The antibacterial study was carried out using a modified agar well diffusion method in order to check the MIC measurement and diameter of zone of inhibiton. Antibacterial activity of compound can be determined against 6 pathogenic strains. The activity was determined at a concentration of 1mg/ml in methanol against 3 gram-positive, *Staphylococcus aureus*, *Salmonella epidermidis*, and *Salmonella citreus* and 3 gram-negative *Escherichia coli*, *Klebsiclla pneumonia* and *Shigella*

flexneri. The microplate assay for measuring antibacterial activity was adapted by incorporating 200µl concentration range of streptomycin as an internal standard (40µg/ml).

2.3.2. MIC (Minimum Inhibitory concentration) measurements

MIC is the lowest concentration to inhibit any kind of visible bacterial growth on culture plates by an antibacterial agent which will inhibit the visible growth of a microorganism after 24h incubation at 37 °C. The most commonly employed methods are the tube dilution method and agar dilution methods. This procedure is a standard assay for antimicrobials. Minimum inhibitory concentrations are important in diagnostic laboratories to confirm resistance of microorganisms to an antimicrobial agent and also to monitor the activity of new antimicrobial agents. The MIC was determined by the broth micro dilution bioassay in 96-well micro titer polystyrene plates; where in six bacterial species, 3 gram-positive (*S. aureus*, *S. epidermidis*, and *S. citreus*) and 3 gram negative (*E. coli*, *K. pneumonia* and *S. flexneri*) were used. The calculation of MICs involves semiquantitative test procedure. It gives an approximate value of minimum concentration of an antibacterial agent required to prevent bacterial growth. The serial dilution method was used for the determination of MICs of these compounds. The method involves the addition of 2µL microbes grown in nutrient broth and 2µL of solutions of varying concentrations of each compound dissolved in methanol to 96 microtitre plates containing 200µL of nutrient broth each. The end result of the test is the minimum concentration of the compound that gives a clear solution, i.e. no visible growth after 24 h in a BOD incubator at 37 °C.

2.3.3. Antifungal study

The aim of study is to assess the antifungal activity of anthraquinone based compounds and to determine the zone of inhibition of synthesized compounds (S1-S8) on fungal strains i.e. *Candida albicans* and *Mucor species*. The samples were dissolved in methanol. Aliquots (10mg/mL) of the each sample were added to assay. The flasks containing 100 mL of sterile growth medium potato dextrose agar (PDA). After vortexing, 50 mL were poured into Petri dishes. The assay was performed by placing a 0.7 cm diameter plug of growing mycelium in the centre of a Petri dish. Three replicates were run simultaneously. The zone of growth inhibition was measured after 24 hours at an incubation of 30°C.

2.4. Superoxide scavenging (Superoxide Dismutase assay)

For antioxidant study by SOD (Superoxide dismutase assay) the reaction mixture containing 1 ml of alkaline DMSO (1 ml DMSO in 10 mM NaOH) and drug (200µg/ml), 100µl of Nitroblue

Tetrazolium (NBT -1mg/ml) was added. NBT was purchased from Hi-Media laboratories. Inhibition of the photo reduction of nitro blue (NBT) was performed to measure the SOD activity. The photo chemically excited riboflavin was first reduced by methionine into a semiquinone, which donated an electron to oxygen to form a superoxide source. The superoxide readily converted the NBT into a purple formazan product. As a result, the SOD activity was inversely related to the amount of formazan formation. MTX was used as a standard. Superoxide radical is generated when sodium hydroxide was added to air saturated DMSO. The generated superoxide remains stable in solution, which can reduce NBT into formazan dye at room temperature and this formazan can be measured at 570 nm. Briefly, to there action mixture containing 1 ml of alkaline DMSO (1 ml DMSO in 10mM NaOH) and drug (200µg/ml), 100µl of NBT (1mg/ml) was added. The scavenging activity was calculated as follows:

$$\text{Superoxide radical scavenging effect (\%)} = [A_0 - A_1 / A_0] \times 100$$

Where A_0 was the absorbance of the control and A_1 was the absorbance in the presence of the sample.

2.5. Spectrophotometric parameters

2.5.1. Materials

UV-Visible absorption spectra measurement was carried out on T80+UV/Vis spectrometer (Shimadzu). The absorption spectra were recorded in wavelength range of 200-800nm. Fluorescence experiments were performed using RF-5301 PC spectrofluorophotometer (Shimadzu).

2.5.2. Sample preparation for UV-Visible and fluorescence spectroscopic studies

Calf thymus (ct) DNA and other chemicals for buffer preparation such as sodium dihydrogen phosphate, disodium hydrogen phosphate were purchased from Sisco research laboratories. The buffer was prepared by dissolving 1.5mM disodium hydrogen phosphate, 0.5mM sodium phosphate, 10mM NaCl and 0.25mM EDTA at pH=7.1 using double distilled water (400 ml). The concentration of ct-DNA was spectroscopically determined by molar extinction coefficient $\epsilon_{\text{DNA}} = 6600\text{M}^{-1}\text{cm}^{-1}$ at 257 nm. The stock solution of mitoxantrone and synthesized series (S1-S8) was prepared by dissolving 1mg of synthesized molecules and MTX in 1ml DMSO. 10µL of each i.e. mitoxantrone and synthesized compounds of S1-S8 series is used to each different concentration of DNA for further study.

2.6. Computational studies

2.6.1. Gaussian protocol

The computational work was carried on Gaussian 98W and Gauss view 6 software tools in order to study the electronic properties of synthesized analogues in comparison to mitoxantrone. The quantum chemical calculations were fully optimized at Density functional theory level of approximation. The optimized HOMO-LUMO structure of analogs were computed by Density functional theory methods with 6-31G d,p. DFT is a widely used approach to compute the geometrical structure of atoms or molecules at electronic level. The hybrid density functional in DFT is B3LYP which stands for Becke, 3-parameter, Lee-Yang-Parr. This method is a low cost method which provides good results. The energy and dipole moment of the optimized structures are obtained from DFT methods.

2.6.2. Autodock

Molecular docking was performed using Autodock 4.0 software <http://autodock.scripps.edu/>. The receptor in docking process is i-moiif sequence d (TC₅) downloaded from RCSB protein data bank bearing PDB code (225d) i.e. the tetrameric DNA structure with protonated cytosine: cytosine base pairs. Molecules were designed using chem sketch (www.acdlabs.com) and saved as mol file. DNA sequence was optimized for energy minimization in Swiss PDB Viewer (SPDBV) version 4.1.0. DNA sequence was loaded and stored as 225d.pdb. The mol file of synthesized analogue was also loaded as pdb in Open BabelGUI. The grid map files were selected directly with 40x40x40 dimensions for searching of ligand with active site of DNA sequence. This way grid parameter was created. Followed by genetic algorithm, the docking parameter used Lamarckian genetic algorithm to predict best fit conformation in docking process. Docking is carried out using Cygwin interface and results were analysed in Pymol 27 software ([ww.pymol.com](http://www.pymol.com)).

3. Result and discussion

3.1. Cytotoxic study

MCF-7 (Human Breast Cancer cell line), PC-3 (Human Prostate Cancer cell line) and Hep 2C (Hela derivative Human cell line) were used with the purpose to confirm the concentration of synthesized 1-substituted (S1-S8) compounds required to cause the damage. Cell lines were treated with different concentration of S1 to S8 series of synthesized compounds for a fixed hours. Mitoxantrone showing cytotoxic effect at lower concentration (1-5µg/ml) for all the cell lines (K-Chyla, Jedrzejczak, Skierski, Kania, & Jozwiak, 2005). 1-substituted anthraquinone

series (S1-S8) compounds showed poor performance for PC-3 cell lines. However little inhibition to MCF-7 cell lines at higher concentration of S2, S3 and S5 compounds has been observed (Fig.1a and 1b) and (Table 1a and 1b). Interestingly S-series showed better action against Hep 2C cell lines. The synthesized compounds S1 and S3 were cytotoxic at 9 μ g/ml while S4 was cytotoxic at 1.008 μ g/ml i.e. better than mitoxantrone at 2.5 μ g/ml.

3.2. Cell cycle analysis

Cell cycle analysis of S3 and S4 compounds of S series against Hela cells for 24 hours produced interesting results. It is well established that mitoxantrone arrests G1 and G2 phases at cell cycle progression and ultimately inhibit the cell growth (Khan, Lal, Kimar, & Khan, 2010). Further it is also confirmed that mitoxantrone also promotes the arrest of S-phase of cell cycle. G1 and G2 are the growth phases in cell cycle analysis whereas S-phase is a synthetic phase where in DNA replication and DNA synthesis takes place. Hence cell goes apoptosis upon treatment with MTX due to inhibition at cell growth phases G1 and G2 alongwith inhibiting the DNA replication/duplication process (S phase). Direct attack on cell regulatory protein is suggested. Further it play vital role in controlling the regulation of G2/M and G1 phases. S4 in accordance to cytotoxic studies on Hep 2C cell lines showing better effect over mitoxantrone i.e. 1.008 μ g/ml and 2.5 μ g/ml respectively (Table 2). Like wise S3/S1 is showing inhibiting action at higher concentration i.e. 9 μ g/ml than MTX 2.5 μ g/ml as per cytotoxic study.

We have carried out flow cytometric study of S4 and S3 compounds only as S3 and S1 are showing almost similar cytotoxic effects. Concentrations of S3 and S4 compounds were taken 10 μ g/ml and 5 μ g/ml respectively as per cytotoxic studies. After examining the data for S4 (Fig. 2) good number of cells are arrested in G₀/G₁ phase i.e. initial phase of cell cycle. Hence all the chemical activities i.e. increase in supply of proteins, doubling in number of cell organelles etc is countered. Biosynthetic activity is very high during G₁ phase which seems to be dropped by 5 % in comparison to control. However the activities in G₂ phase increase by~4.5% i.e. cell accumulation takes place in G₂ phase. 0.1 % cells arrest is observed in S-phase i.e. inhibiting DNA replication mechanism. Similarly for S3 different pattern is observed i.e. variation at G₁ and G₂ phase are 1.3 and 0.1 % respectively in comparison to control. Interestingly S phase is reduced by 1.9 % in comparison to control; indicating the arrest at DNA synthesis i.e. DNA duplication and replication. Hence both the molecules S4 and S3 deregulate the cell cycle which is the primary condition for any drug candidate to be cytotoxic. Further as per literature study G₁ and G₂ check points are mandatory for tumor cell to go for uncontrolled proliferation. Both the

molecules S4 and S3 arrest G₁ and G₂ phase by disturbing biochemical process along with disturbance at S phase i.e. affecting the DNA synthesis/ replication. But some difference in the mechanism of operation of S4 and S3 has been observed during the progression of cell cycle like:

- G₁/G₂ phase were highly disturbed by S4.
- S phase was highly disturbed by S3

It concluded the different mechanism of operation of both the molecules (S3 and S4). Though basic structure of both the compounds i.e. anthraquinone ring and 1-substituted position of side arm is same but small variation in the structural features of side arm affects the cytotoxicity and mechanism of the operation of S3 and S4 at cellular level.

3.3. Antibacterial study and Antifungal studies

Two features (i) -SO₂NH and (ii) -NH-CO are reported to be important for antibacterial and antifungal action. Number of compounds/ drugs are presently in market bearing the said feature, act as an antibacterial and antifungal agents. Synthetic series (S1-S8) is tested against Gram +ve as well as Gram -ve strains in comparison to streptomycin (Table 3). Analogues of (S1-S8) are found to be more active on *K. pneumonia* (Supplementary Fig. II and III; and Supplementary Table D) in comparison to streptomycin. Lack in universality in antibacterial action in comparison to standard drug could be due to hydrophilicity and inability to penetrate in to cell wall of bacteria along with long chains at position 1 on the anthraquinone ring. Likewise the S1 to S8 series showed mild antifungal activity against *Mucor species* and *Candida albicans* (Kang, Fong, & Tsang, 2010) (Supplementary Table II). Hence it is not only the structure features but there position and orientation in a molecule is vital for important biological activities. This requires more detailed structural study while keeping into consideration the pattern shown by S1-S8 series in the said study.

3.4. Antioxidant study

It has been reported by researchers that use of anthraquinone class of drugs in chemotherapy is limited due to their peroxidating activity and production of the free radicals. The activity is initiated by the oxy-reductase enzymes at cellular level which is the main cause of cardiotoxicity. Anthraquinone class of drugs have admiration towards these enzymes as it is likely to go for one electron transfer reaction and produce O₂radicals (oxygen radicals). Comprehensive study have

been carried out and reported in literature on natural and synthetic anthraquinones class of compounds with diversified structural features to check their ability and essential requirement to undergo redox reactions. It has been confirmed that functional group present over the anthraquinone ring favours or disfavours the oxidation-reduction/ free radical formation (Tarasiuk et al, 1998; Alderton, Gross, & Green, 1992; Reszka, Hartley, Kolodziejczyk, & Lown, 1989). However mitoxantrone, a standard reference drug taken in present study, showed poor affinity towards NADH dehydrogenation reaction despite of presence of OH groups at 1 and 4 position and unmodified carbonyl group. Mechanistic reason is not clear but it could be due to presence of aromatic amino group with long chains at 5, 8 substituted positions on the ring. Highest level of flexibility and steric hindrance with protein molecule could be the reason.

Therefore, we have carried out SOD analysis of synthesized series (S1-S8) to evaluate the potential to scavenge O₂ radical production. Interestingly synthesized 1-substituted anthraquinone molecules (S1-S8) were ineffective in stimulating free radical (O₂) oxygen production (Supplementary Table III).

3.5. Spectroscopic confirmation of binding of (S1-S8) compounds with DNA.

3.5.1. UV-Visible spectral studies

Various studies, biochemical as well as biophysical, has confirmed the intercalative mode of binding of mitoxantrone with receptor site i.e. DNA. Mitoxantrone exhibit maximum absorption at 608 and 660 nm and successive addition of ct-DNA leads to hypochromic and bathochromic effect. Intercalative mode of binding is proposed.

Likewise interaction of synthesized 1-substituted anthraquinone molecules (S1-S8) with ct-DNA has been carried out and K_b (binding constant) and ΔG (free energy of binding) has been calculated according to Benesi-Hildebrand equation:

$$\frac{A_0}{A-A_0} = \frac{\epsilon_G}{\epsilon_{H-G}-\epsilon_G} + \frac{\epsilon_G}{\epsilon_{H-G}-\epsilon_G} \frac{1}{K_b[DNA]} \quad (1)$$

A_0 and A are the absorbances of compounds in the absence and presence of DNA, respectively, and ϵ_G and ϵ_{H-G} are the respective absorbance coefficients. K_b is the association/ binding constant. A plot of $A_0/A-A_0$ versus $1/[DNA]$ was constructed, linear fitting of data yielded binding constant (Fig. 3). The values (Table 4) obtained out of experiments are in range with the values reported for interactions of anthracycline molecules with DNA ($K \approx 10^4$ to 10^5 M⁻¹) (Li, Ma, Yang, Guo, & Yang, 2005). All synthesized molecules (S1-S8) show absorption maxima at 420-425 nm. Upon comparing with mitoxantrone, having two maxima at 608-660 nm,

is due to two types of functionalities i.e. OH and NH at 1,4 and 5,8 position respectively. S1-S8 compounds are only 1-substituted and maxima at lower λ could be due to one NH group directly attached to anthraquinone ring along with O=S=O group and absence of OH auxochrome at 1, 4 position of anthraquinone ring. Continuous decrease in absorbance with red shift has been observed for all the molecules (S1-S8) with increasing concentration of DNA. This hypochromic effect is due to interaction between electronic states of (S1-S8) molecules and base pairs of DNA. Slight red shift ($\sim 9 - 24\text{nm}$) in maxima could be due to lack of functional group interaction in internal hydrophobic environment of DNA. All the synthesized molecules (S1-S8) series shows hypochromic effect with red shift upon binding with DNA. This behavior is an indication of partial intercalative mode of binding (Pasternack, Gibbs & Villafranca, 1983; Krugh & Reinhardt, 1975; Lu, Wang, Lv, Zhang, & Liu, 2010). Slightly different pattern of absorption maxima is observed for S5 and S6 molecules. The additional structural feature incorporated in S5 and S6 is CH_3 group at para position of benzene ring A. In case of S5 though intense hypochromic effect with bathochromic shift is observed where as in S6 at high concentration of DNA sharp bathochromic effect has been observed. The only structural difference in S5 and S6 is additional $-\text{CH}_2$ group at (C_n) of (Structure 1). CH_3 group at para position on ring A in S5 could be having some interactions due to fixing of $-\text{NH}-\text{SO}_2-$ group or hydrophobic character leading to steric interactions and allowing $-\text{NH}-\text{SO}_2-$ group for additional interaction with DNA molecule. However in case of S6 initially, if allowed, some polar interaction between the charge functionality of the molecule with DNA bases could be there but at high concentration it was lost. Upon comparing the K_b , the value does not show much difference. However ΔG value for S6 is more than S5. Therefore it confirms some additional interaction of molecule S6 with DNA and finally stabilizing the molecule. But to our surprise same behaviour could not be observed for S7 and S8 where p-substituted $-\text{CH}_3$ is in position at ring A. Upon comparing the structure of S2 and S6 the only difference is para $-\text{CH}_3$ group at ring A while comparing S6 with S7, S5, S8 an additional $-\text{CH}_2$ group is incorporated in the side arm which might have induced extra flexibility to the side chain and ultimately dissimilar behavior of S6 in terms of absorbance maxima and ΔG value.

3.5.2. Fluorescence spectra

Interaction of synthesized compounds (S1-S8) with ct-DNA has been investigated by fluorescence spectroscopic study in order to confirm the intercalative mode of interaction and effect of different structural feature on behavior of molecules (S1-S8) with DNA. The data is

compared with interaction of Mitoxantrone-DNA complex. Mitoxantrone show an excitation maximum at 596nm and emission maxima at 680 nm (Li, Ma, Yang, Guo, & Yang, 2005).

We have carried out experiment by 10 μ M solution of (S1-S8) series and MTX in phosphate buffer solution. λ_{exc} for S1-S8 molecules observed at 390 nm and λ_{em} was in range of 560-565 nm. Similarly for MTX λ_{em} was 600-602nm. Quenching effect is observed in S1-S8 molecule upon binding to DNA. This confirms the hydrophobic interaction of chromophore with DNA bases. In literature, it is proposed that there is lack of substituent interaction of side chain of mitoxantrone with the solvent i.e. water molecules upon binding to DNA and confirms the intercalative mode of binding. In S1-S8 series, no doubt that quenching is shown by all the molecules (S1-S8) i.e. decrease in fluorescence intensity accompanied with shifting toward higher wavelength (\sim 6nm) indicates partial intercalative mode of interaction upon DNA binding. Slight deviation in fluorescence spectra of synthesized compound S1-S8 seems to be due to difference in type of side chain (structure 1 and 2) as red shift is observed at lower D/P ratio. However fluorescence quenching mechanism for S4, S6 and S7 was different. Fluorescence emission spectra of S6 was entirely different from rest of the molecules. Though quenching was observed in fluorescence intensity of S6 but emission spectra is moving fast towards higher λ with rise in DNA concentration. This indicates some additional mode/interaction of ligand with acceptor as observed in absorption spectra (Fig. 3). Though K_{sv} and K_q and ΔG values could not add much on this but their values shows partial intercalative mode of binding (Table 4). However behaviour of S1-S8 series molecule in emission spectra clearly indicates that extension of side arm with more hydrophobic groups along with polar functionality i.e. $-\text{NH}-\text{SO}_2-$ would leads to additional flexibility at side chain and ultimately additional interactions (Awasthi, Dogra, & Barthwal, 2013; Khan, Islam, Yennamalli, Sultan, Subbarao and Khan, 2008).

The fluorescence quenching constant, K_{sv} is evaluated using Stern-Volmer equation:

$$F_0/F = 1 + K_{sv} [\text{DNA}] \quad (2)$$

Where F_0 and F are the fluorescence intensities in the absence and presence of DNA respectively, $[\text{DNA}]$ is total concentration of ct-DNA, K_{sv} is Stern Volmer quenching constant (a measure of quenching efficiency by DNA). K_{sv} is obtained by plot of F_0/F versus $[\text{DNA}]$. Using a typical fluorescence life time of 0.2×10^{-9} s; the corresponding biomolecular quenching constant K_q is

calculated. The binding constant K_b and binding stoichiometry (n) of the compound has been determined using following equation:

$$\text{Log } (F_0 - F)/F = \text{log } K_b + n \text{ log } [Q] \quad (3)$$

Where Q is quencher concentration i.e. $[Q] = [\text{DNA}]$.

Further the total binding energy changes were calculated according to standard Gibbs equation:

$$\Delta G^0 = -RT \ln K_b \quad (4)$$

where R and T refers to gas constant and temperature in kelvin respectively. All the parameters are mentioned in (Table 5) and fluorescence spectra are shown in (Fig. 4). All molecules (S1-S8) series showing linear straight line graph of Stern-Volmer plot. Therefore, only one type of quenching process is operational i.e. either static or dynamic (Lakowicz, pp. 239-240; Zhong, Yu, Huang, Ni, & Liang, 2001). S4 is showing better cytotoxic activity in comparison to Mitoxantrone and fluorescence spectrum of S4 differs than rest (S1, S2, S3, S5, S6, S7 and S8) as well as Mitoxantrone. Quenching is slow and shift in fluorescence intensity toward right i.e. at higher wavelength. Therefore, in addition to partial intercalative mode of interaction, molecule is also undergoing additional mode of interaction with DNA molecule by involving its polar side chains bearing $-\text{NH}-\text{CO}_2-$ and $-\text{NH}-\text{SO}_2-$ functional groups (Dogra, Awasthi, Nair, & Barthwal, 2013).

3.6. Molecular modelling

3.6.1. Electronic properties of synthesized (S1-S8) and MTX

In order to correlate the binding mechanism and cell killing potential of S1-S8 series with their electronic properties; detailed quantum chemical study has been carried out using DFT/6-31G (d,p) method. Molecular orbitals and atomic charges are calculated. Results were compared with MTX. The highest occupied molecular orbital (HOMO) represents the ability to donate an electron while lowest unoccupied molecular orbital (LUMO) represents the ability to accept an electron hence corresponds to ionization potential and electron affinity respectively. The HOMO-LUMO calculation has been carried out and graphical representation of movement of charge, dipole moment and energy indicates the large electronic difference between synthesized series (S1-S8) (Fig. 5). For the stability of the structure of the molecule, energy gap between the HOMO and LUMO orbitals is an important parameter. The molecule with smaller energy gap have higher reactivity and low kinetic stability and considered to be soft molecule (Shukla,

Yadava, & Roychoudhury, 2015). Energy gap (a.u.) in MTX is higher than rest of synthesized compounds of the series (S1-S8). At the same time dipole moment of synthesised series (S1-S8) is higher than MTX (Table 6). Therefore it can be concluded that due to small difference in HOMO-LUMO of S1-S8 series along with high dipole moment; synthesized molecules (S1-S8) can be easily reduced. At the same time due to instability in the conformation might lead to fall in cytotoxicity in comparison to MTX. As per electronic study S1 is quite comparable with mitoxantrone in terms of energy gap but S3 and S4, are claimed to be comparable to MTX in terms of ct-DNA binding and cytotoxic study (Table 1a). Moreover upon comparing the dipole moment of synthesized molecules (S1-S8) it is interesting to note that since all the synthesized molecules (S1-S8) differs at R₁ and R₂ (Structure1); the dipole moment of S1 and S5 (R₁= H and R₂= CH₃) is comparable to MTX, whereas rest of compounds with (R₁= H and R₂= CH₃) i.e. S3 and S7; S2 and S6; S4 and S8 large variation in dipole moment is observed. In majority of cases, X component of dipole moment is going -ve to +ve and adding up in the total resultant value (Fig. 5). However variation in R₂, specifically, in S4, addition of CH₂ group in the side chain at position 1 raised the direction of electrical dipole value to +8.2 which is completely different from MTX. Interestingly S4 is more cytotoxic at lesser micro molar concentration than MTX i.e. 1.008µg/ml and 2.5µg/ml respectively (Table 1a). Therefore, some additional/different mechanism of operation seems to be followed while drug interacting with receptor.

3.6.2. Molecular docking details

Computational docking tool is used to understand the binding interaction of synthesized molecules (S1-S8) with telomeric sequence. The binding energy, binding interactions, hydrogen bond length (Å) are listed in (Supplementary Table IV). The orientation and hydrogen bond length is shown in (Fig. 6). It is well known that mitoxantrone interact with DNA via interfering the telomeric activity. They have also shown to inhibit telomeric activity (Barthwal, Tripathi, Pradeep, 2015).; Searle, & Balkwill, 2006; Phan, & Mergny, 2002; Kim et al, 1994, Tripathi, S., Pradeep, P, Tarikere & Barthwal Ritu, 2016). Telomere are proposed to be “biological clock” in order to determine the proliferative activity of the human cells (Cairns, Michalitsi, Jenkins, & Mackay, 2002). Mitoxantrone and various synthesized analogue has been studied to intercalate at telomeric junction of the DNA (Neidle, & Parkinson, 2002; Waller, Sewitz, Hsu, & Balasubramanian, 2009; Yang, & Issa, 2003). Based on these lines we have carried out docking study of synthesized series (S1-S8) along with mitoxantrone on with d (TC₅). Data is tabulated

in (Supplementary Table IV). Not much of the difference in ΔG_b (Kcal/mol) could be observed. However variation in K_i can be seen for synthesized series (S1-S8) and MTX. Therefore it is concluded that synthesized series (S1-S8) and MTX binds to i-motifs. However same could be validated only after doing experimental studies for synthesized series hence would be reported subsequently.

4. Conclusion

Anthracycline class of drugs are most commonly used chemotherapeutic agents. Number of analogues of this class of compounds are reported but Adriamycin, Daunomycin and Mitoxantrone are presently in use in cancer hospitals. Mitoxantrone is proposed to be less cardiotoxic over Adriamycin and Daunomycin. Further 1, 4 substituted diamino alkyl chains on anthraquinone chromophore are proposed to be important along with 5, 8 substituted -OH groups (Structure 2) for desired biological activity. Anthraquinone ring facilitate the docking of the molecule in the DNA double helix via intercalation however 1,4 diaminoalkyl side arm interacts with DNA and imparts biological activity; hence declared to be pharmacophoric group (Konopa, 2001). In present research paper we have synthesized series of 1-substituted anthraquinone compounds. 1-substituted side arm is modified by incorporating sulphonamide and amide functionalities. Sulphonamide and amide functionalities are proved to show antiproliferative activities in some cell lines as per literature study. All the synthesized molecules in series (S1-S8) having 1-substituted anthraquinone ring but molecules differs in structure and functional groups at the side arm. Comprehensive biological and spectrophotometric studies has been carried out on synthesized molecules (S1-S8) in comparison to the Mitoxantrone. Significant cytotoxic activity has been observed over Hela cell lines and one of the molecule S4 is showing better activity over Mitoxantrone. Cell cycle analysis of S3 and S4 molecules indicates the arrest of cell cycle at G1 and G2 phases. Similarly partial intercalation mode of binding of all the synthesized molecules (S1-S8) is proposed in comparison to Mitoxantrone on the basis of spectrophotometric study. Antioxidant study could not conclude any result however small energy gap with high dipole moment of synthesized molecule (S1-S8) than Mitoxantrone has been observed using DFT/6-31G (d,p) method. Molecules (S1-S8) are proposed to be reactive and will facilitate in formation of charge transfer complexes. Further synthesized series are proposed to be good i-motif inhibitor using docking tools. In present study, we conclude that 1,4 (OH) position and 5,8 diaminoalkyl residue on anthraquinone ring is not mandatory

requirement for molecule to be anticancer agent, whereas structure and functionality over side arm is proposed to be important to mark the desired biological activity. Further same would be confirmed only after we report synthesis of (2); (3); (1,4); (1,8) and (1,5) substituted anthraquinone with sulfonamide and amide functionality bearing side arms. Chromophore modification with 1 and 1, 4 substitution with 1-[1-oxo-3-phenyl-(2-benzosulfonamide)-propyl amido] – anthracene-9, 10-Dione arm will finally confirm the same, hence, will be reported subsequently. Further studies on thermal stability of DNA on binding to different ligands S1-S8 are expected to provide further insight into the binding mechanism. We have also carried out antibacterial and antifungal affects of synthesized series. S1-S8 molecules showed mild activities for antibacterial and antifungal actions.

Acknowledgements

This work was supported by the Department of Science & Technology, Government of India, New Delhi, under grant no. SR/WOS-A/CS-1030/2015 in Women Scientist Scheme and CSIR UGC-JRF fellowship. Authors are Thankful to SAIF lab, Punjab University, Chandigarh for NMR and ESI-MS experiments. *In vitro* SRB assay for anti-cancer activity was carried out at Anti-Cancer Drug screening facility (ACDSF) at ACTREC, Tata Memorial Centre, Navi Mumbai. Authors acknowledge the cell cycle analysis work at Pharmacology and Toxicology lab, Food and Nutraceuticals Division, CSIR-IHBT, Palampur. Authors also acknowledge the support extended by Dr. S.S. Kanwar and his group, Department of Biotechnology, Himachal Pradesh University, Shimla for MTT assay and antibacterial studies. The facilities provide by National Institute of Technology, Hamirpur are highly acknowledged. The paper is original research of authors and also filed as a patent (Indian patent application no. 201711026145).

References

Adachi, C., Zhang, Q., Kuwabara, H., Potscavage, W. J., Huang, S., Hatae Y. & Shibata, T. (2014). Anthraquinone based intramolecular charge-transfer compounds: Computational molecular design, thermally activated delayed fluorescence, and highly efficient red electroluminescence. *Journal of American Chemical Society*, 136, 18070-18081. [dx.doi.org/10.1021/ja510144h](https://doi.org/10.1021/ja510144h).

Alderton, P. M., Gross, J. & Green, M. D. (1992). Comparative study of doxorubicin, mitoxantrone, and epirubicin in combination with ICRF-187 (ADR-529) in a chronic cardiotoxicity animal model. *Cancer Research*, 52, 194-201.

Alsughayer, A., Elassar, A-Z. A., Mustafa, S. & Sagheer, F. A. (2011). Synthesis, structure analysis and antibacterial activity of new potent sulfonamide derivatives. *Journal of Biomaterials and Nanobiotechnology*, 2, 144-149. doi:10.4236/jbnb.2011.22018.

Awasthi, P., Dogra, S. & Barthwal, R. (2013). Multispectroscopic methods reveal different modes of interaction of anticancer drug mitoxantrone with Poly (dG-d C). Poly (dG-dC) and Poly (dA- dT). Poly (dA- dT). *Journal of Photochemistry and Photobiology B: Biology*, 127, 78-87. <https://doi.org/10.1016/j.jphotobiol.2013.07.023>.

Bailly, C., Routier, S., Bernier, J-L. & Waring, M-J. (1996). DNA recognition by two mitoxantrone analogues: influence of the hydroxyl groups. *FEBS Letters*, 379, 269-272. doi/10.1016/0014-5793(95)01528-0.

Balasubramanian, S. & Neidle, S. (2009). G-Quadruplex nucleic acids as therapeutic agents. *Current opinion in chemical biology*, 345-353.

Barthwal, R., Tripathi, S., Pradeep, P, Tarikere (2015). 123 NMR study of interaction of mitoxantrone to G-quadruplex sequences leading to stabilization and inhibition of telomerase enzyme. *Journal of biomolecular structure and Dynamics*, 33 doi/org/10.1080/07391102.2015.1032756

Beziane, A., Terme, T. & Vanelle, P. (2005). An electron transfer approach to the preparation of highly functionalized anthraquinones. *Molecules*, 10, 289-294. doi:10.3390/10010289.

Cairns, D., Michalitsi, E., Jenkins, T. C. & Mackay, S. P. (2002). Molecular modelling and cytotoxicity of substituted anthraquinones as inhibitors of human telomerase. *Bioorganic & Medicinal Chemistry*, 10, 803-807. doi: [10.1016/S0968-0896\(01\)00337-6](https://doi.org/10.1016/S0968-0896(01)00337-6).

Cheng-Zee, Robert, K.-Y., Cheng, C. C. (1978). Antineoplastic agents. Structure-activity relationship study of bis-(substituted amino-alkylamino) anthraquinones. *Journal of Medicinal Chemistry*, 21, 291-294. doi:10.1021/jm00201a012.

Chung, Y-L., Pan, C-H., Liou, W-H., Sheu, M-J., Lin, W-H., Chen, T-C., Huang, H-S. & Wu, C-H. (2014). NSC746364, a G-quadruplex- stabilizing agent, suppresses cell growth of A549 Human lung cancer cells through activation of the ATR/ Chk1- dependent pathway. *Journal of Pharmacological Sciences*, 124, 7-17. doi: 10.1254/jphs.13096FP.

Collier, D. A. & Neidle, S. (1988). Synthesis, Molecular modelling, DNA binding and antitumor properties of some substituted amidoanthraquinones. *Journal of Medicinal Chemistry*, 31, 4, 847-857. doi:10.1021/jm00399a028.

Dogra, S., Awasthi, P., Nair, M. & Barthwal, R.(2013). Interaction of anticancer drug mitoxantrone with DNA hexamer sequence d-(CTCGAG)₂ by absorption, fluorescence and circular dichromism. *Journal of Photochemistry and photobiology B: Biology*, 123 , 48-54. doi 10.1016/j.j photobiol.2013.03.015.

Ella, D. A. A. E., Ghorab, M. M., Heiba, H. I. & Soliman, A. M. (2011). Synthesis of some new thiazopyrane and thiazolopyranopyrimidine derivatives bearing a sulfonamide moiety for evaluation as anticancer and radiosensitizing agents. *Medicinal Chemistry Research*, 21: 2395–2407. doi 10.1007/s00044-011-9751-9.

Freccero, M., Percivalle, C., Sissi, C., Greco, M. L., Musetti, C., Mariani, A., Artese, A. Costa, G., Perrore, M. L. & Alcaro, S. (2014). Aryl ethynyl anthraquinones: a useful platform for targeting telomeric G-quadruplex structures. *Organic and Biomolecular Chemistry*, 12, 3744-3754. doi:10.1039/c4ob00220b.

Fukuoka, K., Usuda, J., Iwamoto, Y., Fukumoto, H., Nakamura, T., Yoneda, T., Narita, N., Saijo, N. & Nishio, K. (2001). Mechanisms of action of the novel sulfonamide anticancer agent E7070 on cell cycle progression in human non-small cell lung cancer cells. *Investigational New Drugs*, 19, 219-227. <https://doi.org/10.1023/A:1010608317361>.

Guidi, A., Canfarini, F., Giolitti, A., Pasqui, F., Pestellini, V. & Arcamone, F. (1994). Synthesis of new antitumor anthracyclines: Derivatives bearing a fluorine substitution at position 8 or 10. *Pure and Applied Chemistry*, 66, 2319-2322. doi.10.1351/pac199466102319.

Horn, D. E., Leonard, M. E., Fischl, A. J., Gray, M., Clark, D. W., A- Mahlock, T. & Sader, C. N. (2000). Synthesis of symmetrically 1, 4- bis [(aminoalkyl) amino]-5, 8- Dimethylantracene-9, 10-diones. *ARKIVOC*, 1, 876-881.

Huang, H-S., Chiu, H-F., Lu, W-C. & Yuan, C-L. (2005). Synthesis and antitumor activity of 1, 8-Diaminoanthraquinone derivatives. *Chem. Pharm. Bull.*, 53, 9, 1136-1139. doi:

Kang, K., Fong, W-P. & Tsang, P. W-K. (2010). Novel antifungal activity of purpurin against *Candida* species in vitro. *Medical Mycology*, 48, 904-911. DOI: 10.3109/13693781003739351.

Kim, N. W., Piatyszek, M. A., Prowse, K. R., Harley, C. B., West, M. D., Ho, P. L. C., Coviello, G. M., Wright, W. E., Weinrich, S. L. & Shay, J. W. (1994). Specific association of human telomerase activity with immortal cells and cancer. *Science* 266, 2011-2015.

Khan, S.N., Lal, S.K., Kimar, P. & Khan, A. U. (2010). Effect of Mitoxantrone on proliferation dynamics and cell- cycle progression. *Bioscience Reports*, 30, 375-381. doi 10.1042/BSR20090119.

Konopa, J. (2001). Antitumor acridines with diaminoalkylo pharmacophoric group. *Pure Applied Chemistry*, 73, 1421-1428. doi:10.1351/pac200173091421.

Khan, S.N., Islam, B., Yennamalli, R., Sultan, A., Subbarao, N., Khan. A.U. (2008). Interaction of mitoxantrone with human serum albumin: Spectroscopic and molecular modelling studies. *European journal of pharmaceutical sciences*, 35, 371-382.

Krapcho, A. P., Getahun, Z., Avery, K. L., Vargas, K. J. & Hacker, M. P., (1991). Synthesis and antitumor evaluations of symmetrically and unsymmetrical substituted 1,4- bis [(aminoalkyl) amino] anthracene-9,10- diones and 1,4- bis [(aminoalkyl)amino]-5,8-dihydroxyanthracene-9,10 diones. *Journal of Medicinal Chemistry*, 34, 2373-2380. doi: 10.1021/jm00112a009.

Krugh, T. R. & Reinhardt, C. G. (1975). Evidence for Sequence Preferences in the Intercalative Binding of Ethidium Bromide to Dinucleoside Monophosphates. *Journal of Molecular Biology* 97, 133-162. doi:10.1016/80022-2836(75)8031-3.

K-Chyla, A., Jedrzejczak, M., Skierski, J., Kania, K. & Jozwiak, Z. (2005). Mechanisms of induction of apoptosis by anthraquinone anticancer drugs aclarubicin and mitoxantrone in

comparison with doxorubicin: Relation to drug cytotoxicity and caspase-3 activation. *Apoptosis*, 10, 1497-1514. DOI: 10.1007/s10495-005-1540-9.

Lakowicz, I. R.. *Principles of fluorescence spectroscopy*. Kluwer Academic, New York, 239-240.

Li, N., Ma, Y., Yang, C., Guo, L. & Yang, X. (2005). Interaction of anticancer drug mitoxantrone with DNA analyzed by electrochemical and spectroscopic methods. *Biophysical Chemistry*, 116, 199-205. doi:10.1016/j.bpc.2005.04.009.

Lu, Y., Wang, G-K, Lv, J., Zhang, G-S. & Liu, Q-F. (2010). Studies on the interaction of an anthracycline disaccharide with DNA by spectroscopic techniques and molecular modelling. *Journal of Fluorescence*, 21, 409–414. DOI 10.1007/s10895-010-0729-7.

Murdock, K. C., Child, R. G., Fabio, P. F., Angier, R. B. (1979). Antitumor agents. 1. 1, 4- Bis [(aminoalkyl) amino]-9, 10- anthracenediones. *Journal of Medicinal Chemistry*, 22, 9, 1024-1029. doi: 10.1021/jm00195a002.

Neidle, S. & Parkinson, G. (2002). Telomere maintenance as a target for drug discovery. *Nature Reviews Drug Discovery*, 1, 383-393.

Nor, S. M. M., Sukari, M. A. H. M., Azziz, S. S. S. A., Fah, W. C., Alimon, H. & Juhan, S. F. (2013). Synthesis of new cytotoxic aminoanthraquinone derivatives via nucleophilic substitution reactions. *Molecules*, 18, 8046-8062. doi:10.3390/molecules18078046

Pasternack, R. F., Gibbs, E. J., & Villafrancas J. J. (1983). Interactions of Porphyrins with Nucleic Acids. *Biochemistry* 22, 5409-5417. doi: 10.1021/bi00292a024.

Phan, A. T. & Mergny, J-L. (2002). Human telomeric DNA: G-quadruplex, i-motif and Watson-crick double helix. *Nucleic acids research* 30, 21, 4618-4625. doi:10.1093/nar/gkf597. x

Reszka, K., Hartley, J. A., Kolodziejczyk, P. & Lown, J. W. (1989). Interaction of the peroxidase- derived metabolite of mitoxantrone with nucleic acids. Evidence for covalent binding of ¹⁴C-labeled drug. *Biochem Pharmacology*, 23, 4253-4260. doi: 10.1016/0006-2952(89) 90523.

Routier, S., Bernier, J-L., Catteau, J-P., Riou, J-F. & Bailly, C. (1998). Synthesis, DNA binding, topoisomerase III inhibition and cytotoxicity of two guanidine- containing anthracene-9, 10 diones. *Anticancer Drug Design*, 13, 407-415.

S-Aliabadi, H., Tabarzadi, M. & Zarghi, A. (2004). Synthesis and cytotoxic evaluation of two novel anthraquinone derivatives. *FARMACO*, 59, 645-649. Doi: 10.1016/j.farmac.2004.03.006.

Searle, M. S. & Balkwill, G. D. (2006). DNA Qadruplex-ligand recognition: Structure and Dynamics in: S. Neidle, S. Balasubramanian *Quadruplex nucleic acids*, RSC Publishing, Cambridge, 131-149.

Shukla, B. K., Yadava, U., Roychoudhury, M. (2015). Theoretical explorations on the molecular structure and IR frequencies of 3-phenyl-1-tosyl-1H-pyrazolo [3, 4-d] pyrimidin-4-amine in view of experimental results. *Journal of Molecular Liquids*, 212, 325-330. <http://dx.doi.org/10.1016/j.molliq.2015.09.021>

Sissi, C., Moro, S., Zagotto, G., Ellis, M., Krapcho, A. P., Menta, E. & Palumbo, M. (1999). Binding of bis-substituted 2-aza-antracenedione regioisomers to DNA: effects of the relative positioning of the side chains. *Anticancer Drug Design*, 14, 265-274.

Skehn P., Storeng, R., Scudiero, A., Monks, J., McMohan, D., Vistica, D., Jonathan, T. W., Bokesch, H., Kenney, S., Boyd, M. R. (1990). New colorimetric cytotoxicity assay for anticancer drug screening. *J. Natl. Cancer Inst.*, 82, 1107. Doi: 10.1093/jnci/82.13.1107.

Supuran, C. T., Briganti, F., Tilli, S., Chegwiddden, W. R. & Scozzafava, A. (2001). Carbonic anhydrase inhibitors: Sulfonamides as antitumor agents. *Bioorganic and Medicinal Chemistry*, 9, 703-714. Doi: 10.1016/s0968-0896(00)00288-1.

Tan, C., Noronha, R de, Devi, N. S., Jabbar, A. A., YLiu, S. K, , Mooring, S. R., Nicolaou, K. C., Wang, B., Mair, E. G. V. (2011). Sulfonamides as a new scaffold for hypoxia inducible factor pathway inhibitors. 21 (18), 5528-5532. <https://doi.org/10.1016/j.bmcl.2011.06.099>.

Tarasiuk, J., Gobis, K. T., Stefanska, B., Dzieduszycka, M., Priebe, W., Martelli, S. & Borowski, E. (1998). The role of structural factors of antraquinone compounds and their quinone- modified analogues in NADH dehydrogenase- catalysed oxygen radical formation. *Anticancer Drug Design*, 13, 923-939.

Tripathi, S., Pradeep, P, Tarikere & Barthwal Ritu. (2016). Molecular Recognition of Parallel DNA Quadruplex d (TTAGGGT)₄ by Mitoxantrone: Binding with 1:2 Stoichiometry Leading to Thermal Stabilization and Telomerase Inhibition. CHEM BIO CHEM communications, 17, 554-560. doi: 10.1002/cbic.201500588 .

Vanicha Vichai & Kanyawim Kirtikara (2006). Sulforhodamine B colorimetric assay for cytotoxicity screening. Nature Protocols 1, 1112 – 1116. <https://doi.org/10.1038/nprot.2006.179>.

Vatsal, M., Devi, V. & Awasthi, P. (2018). Structural and theoretical study of 1-[1-oxo-3-phenyl-(2-benzosulfonamide)-propyl amido] – anthracene-9, 10-Dione to be i-motif inhibitor. Journal of Molecular structure, 1157, 230-238. <https://doi.org/10.1016/j.molstruc.2017.12.054>

Waller, Z. A. E., Sewitz, S. A., Hsu, S-T. D., Balasubramanian, S. (2009). A small molecule that disrupts G-quadruplex DNA structure and enhances gene expression. Journal of American chemical society, 131, 12628-12633. doi: 10.1021/ja901892u.

Wei, B-L., Wu, S-H., Chung, M-I., Won, S-J. & Lin, C-N. (2000). Synthesis and cytotoxic effect of 1, 3-dihydroxy-9, 10-anthraquinones derivatives. European Journal of Medicinal Chemistry, 35, 1089-1098. [https://doi.org/10.1016/S0223-5234\(00\)01190-9](https://doi.org/10.1016/S0223-5234(00)01190-9).

Wright. E.P., Day. H. A. Ibrahim. M.A., Kumar. J., Boswell. L.J.E, Huguin. C, Stevenson. C.E.M, Pors. K and Waller. Z.A.E., (2016). Mitoxantrone and Analogues Bind and Stabilize i-Motif Forming DNA Sequences. Nature, doi: 10.1038/srep39456.

Yang, A. S. & Issa, J-P. J. (2003). A Hypomethylating agent. Cancer Biology and Therapy, 264-265.

Zagotto, G., Moro, S., Uriate, E., Ferrazzi, E., Palu, G. and Palumbo, M. (1997). Amido analogs of mitoxantrone: physico-chemical properties, molecular modelling, cellular effects and antineoplastic potential. Anti-Cancer Drug Design, 12, 99-112.

Zagotto, G., Sissi, C., Gatto, B., Palumbo, M. (2004). Aminoacyl- analogues of mitoxantrone as novel DNA-damaging cytotoxic agents. ARKIVOC, 204-218. Doi: <http://sci-hub.tw/http://dx.doi.org/10.3998/ark.5550190.0005.519>

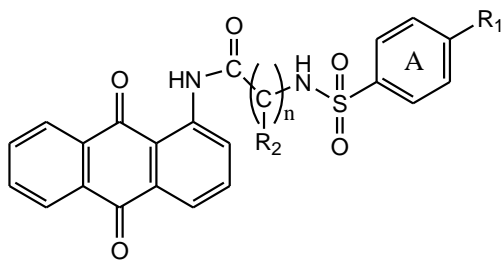
Zagotto, G., Supino, R., Favini, E., Moro, S. & Palumbo, M. (2000). New 1, 4- anthracene -9, 10-dione derivatives as potential anticancer agents. *IL FARMACO*, 55, 1-5. doi:10.1016/s0014-827x(99)00091-9.

Zhang, J., Redman, N., Litke, A. P., Zeng, J., Zhan, J., Chan, K. Y., Chang, C-W. T. (2011). Synthesis and antibacterial activity study of a novel class of cationic anthraquinone analogs. *Biorganic and Medicinal Chemistry*, 19, 498-503. doi:10.1016/j.bmc.2010.11.001.

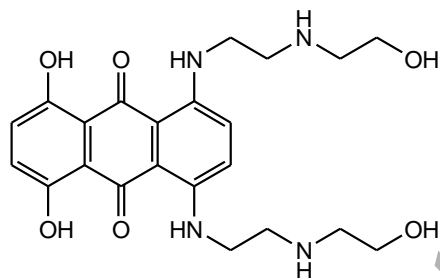
Zhong, W., Yu, J. S., Huang, W. L., Ni, K. Y. & Liang, Y. Q. (2001). Spectroscopic studies of interaction of chlorobenzylidene with DNA. *Biopolymers*, 62, 315-323. doi:10.1002/bip.10001.

Zuravka, I., Sobic, A., Gatto, B. & Gootlich, R. (2015). Synthesis and evaluation of a bis-3-chloropiperidine derivative incorporating an anthraquinone chromophore. *Biorganic and Medicinal Chemistry Letters*, 25, 4606-4609. <http://dx.doi.org/10.1016/j.bmcl.2015.08.042>.

Accepted Manuscript



$R_1 = \text{CH}_3$ (S5, S6, S7 & S8)
 $R_1 = \text{H}$ (S1, S2, S3 & S4)
 $R_2 = -\text{CH}_2\text{C}_6\text{H}_5$ & $-\text{CH}(\text{CH}_3)_2$ (S1, S3, S4, S5, S7 & S8)
 $n = 2$ (S2 & S6)



Structure 1. Basic structure of synthesized compounds. Structure 2. Structure of Mitoxantrone.

Accepted Manuscript

Table 1a. Cytotoxic studies on Hep2C cell lines (Hela Derivative)*

Hep-2C (Hela cells) Human cervix carcinoma	IC ₅₀ value (Concentration of an inhibitor where the response (or binding) is reduced by half)
MTX	2.5µg/ml
S-1	9µg/ml
S-2	NE
S-3	9µg/ml
S-4	1.008µg/ml
S-5	NE
S-6	NE
S-7	N
S-8	NE

NE= Not effective.

* Cervix carcinoma at 24 h, as determine by 3-(4,5-dimethylthiazol-2-yl)-2,5-diphenyl tetrazolium bromide assay.

Accepted Manuscript

Table 1b. Measurement of Potential Cytotoxicity of (S1-S8) series by Sulforhodamine B (SRB) Assay on MCF-7 (Human breast cancer cell line) and PC-3 (Human prostate cancer cell line).

Compounds	MCF-7 (GI ₅₀ = Concentration of drug causing 50% inhibition of cell growth) (µg/ml)	PC-3 (GI ₅₀ = Concentration of drug causing 50% inhibition of cell growth)
S1	<10	NE
S2	41.2	NE
S3	58.0	NE
S4	NE	NE
S5	>80	NE
S6	NE	NE
S7	-	NE
S8	NE	NE
MTX	<10	<10

Accepted Manuscript

Table 2. Cell cycle analysis

Sample	Population (% Cell distribution)		
	G ₀ /G ₁	S	G ₂ /M
Control	73.6	17.4	8.44
S4 (5μg/ml)	68.5	17.3	12.1
S3 (10μg/ml)	74.9	15.4	8.38

Accepted Manuscript

Table 3. Minimum inhibitory concentration against clinically isolated micro-organisms (lg/ml).

S.no	Compounds	Gram-positive			Gram- negative		
		S.aureus	S.epidermidis	S.citrus	E.coli	S.flexneri	K.pneumoniae
1	S1	+	3.06	+	12.25	6.12	6.12
2	S2	24.5	6.12	12.25	12.25	6.125	0.76
3	S3	+	12.25	+	6.12	1.53	1.53
4	S4	12.25	3.06	3.06	24.5	6.12	1.53
5	S5	24.5	3.06	12.25	24.5	6.12	0.76
6	S6	24.5	0.76	12.25	24.5	6.12	0.76
7	S7	24.5	12.25	6.12	12.25	6.12	0.76
8	S8	12.2	12.2	6.12	12.2	6.12	0.76
9	Streptomycin	3.06	0.76	2.15	3.06	0.76	6.12

Accepted Manuscript

Table 4. Binding constant (K_b) and ΔG of 1-substituted anthraquinone compounds (S1-S8) and MTX.

Compounds	K_b (M^{-1})	ΔG (KJ/mol)
S1	9.92×10^4	-28.509
S2	2.84×10^4	-25.409
S3	1.23×10^5	-29.042
S4	8.36×10^3	-22.339
S5	4.86×10^4	-26.741
S6	2.9×10^3	-19.755
S7	6.69×10^4	-27.533
S8	5.26×10^4	-26.94
MTX	1.52×10^5	-29.57

Accepted Manuscript

Table 5. Binding constant (K_b), Stern Volmer constant (K_{sv}), quenching constant (K_q), specific sites (n) and free energy change (ΔG) of 1-substituted anthraquinone compounds (S1-S8) and MTX.

Compounds	K_{sv} (M^{-1})	K_q ($M^{-1} s^{-1}$)	K_b (M^{-1})	n	ΔG (KJ/mol)
S1	9.45×10^4	4.73×10^{14}	2.84×10^5	1.065	-31.12
S2	3.86×10^4	1.93×10^{14}	6.81×10^4	1.067	-27.57
S3	8.57×10^4	4.29×10^{14}	7.09×10^4	0.972	-27.68
S4	4.98×10^3	2.49×10^{13}	1.091×10^3	0.834	-17.33
S5	5.35×10^4	2.67×10^{14}	1.35×10^4	0.857	-23.57
S6	3.59×10^4	1.79×10^{14}	1.004×10^4	0.869	-22.83
S7	2.69×10^4	1.34×10^{14}	3.94×10^4	1.026	-26.22
S8	4.3×10^4	2.15×10^{14}	5.3×10^4	0.983	-26.97
MTX	8.96×10^4	4.48×10^{14}	3.48×10^5	1.125	-31.62

Accepted Manuscript

Table 6. Total energy, degree of freedom and electric dipole moment.

Compounds	Energy (Hartree)	DFT(6-31G (d,p) Dipole Moment (Debye)	Energy gap (a.u.)
MTX	-1525.7251	1.66 (x= -1.0727, y= -0.2746, z= -1.2495)	-0.302
S-1	-1845.7423	5.06 (x=1.7479, y= -4.7236, z= -0.5088)	-0.231
S-2	-1762.0184	6.38 (x=6.3259, y= -0.8614, z=0.1724)	-0.057
S-3	-1835.8698	6.35 (x=1.4122, y=6.0975, z=1.0888)	-0.03
S-4	-1718.5155	9.67 (x=8.2619, y= -4.9086, z= -1.1295)	-0.042
S-5	-2037.7217	6.42 (x=6.0848, y=1.1114, z= -1.7200)	-0.048
S-6	-1799.6466	15.71 (x=15.6710, y= -1.1302, z=0.151)	-0.029
S-7	-1882.4946	2.03 (x= -0.63358, y= -1.4244, z= -1.302)	-0.01
S-8	-1765.1083	4.58 (x= -4.574, y=0.267, z=2.0702)	-0.006

Accepted Manuscript

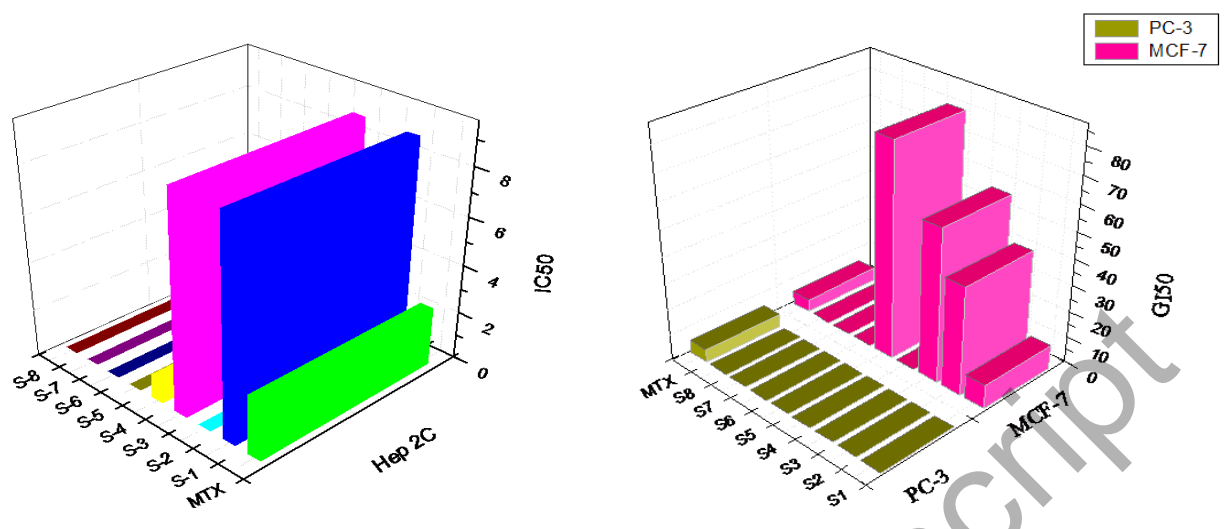


Fig. 1a. IC₅₀ for Hep 2C cancer cell assay

Fig. 1b. GI₅₀ for MCF-7 and PC-3 cancer cell assay

Accepted Manuscript

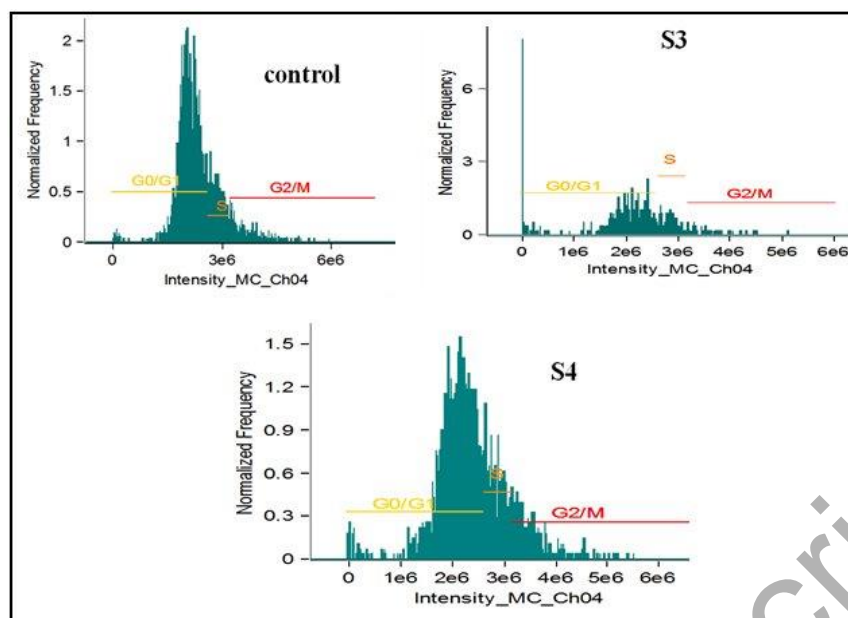
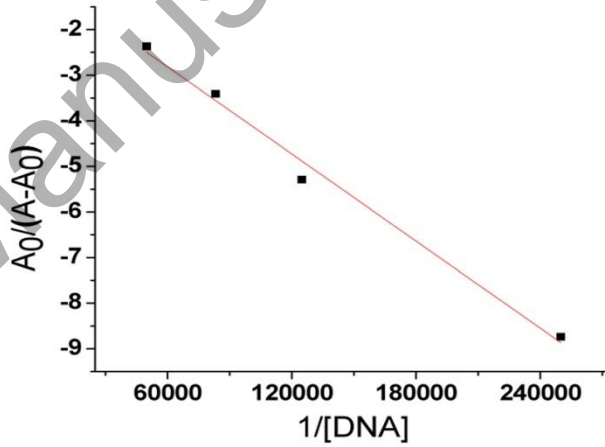
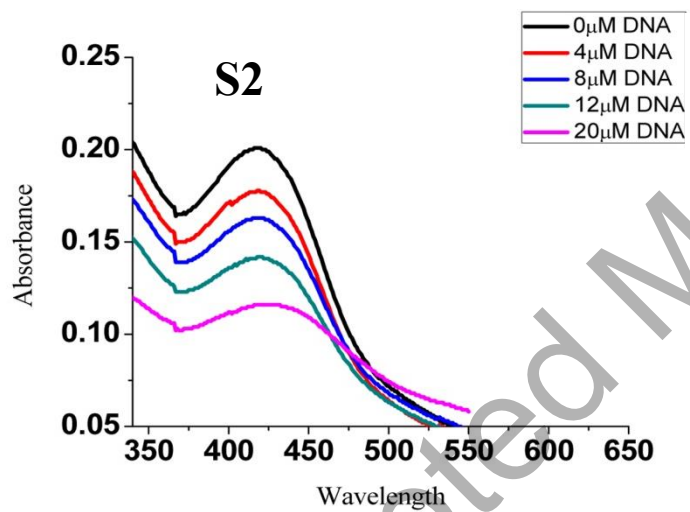
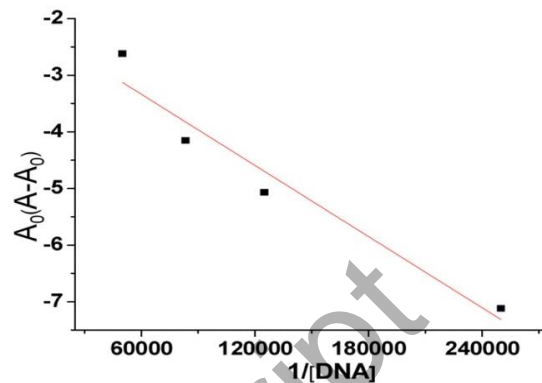
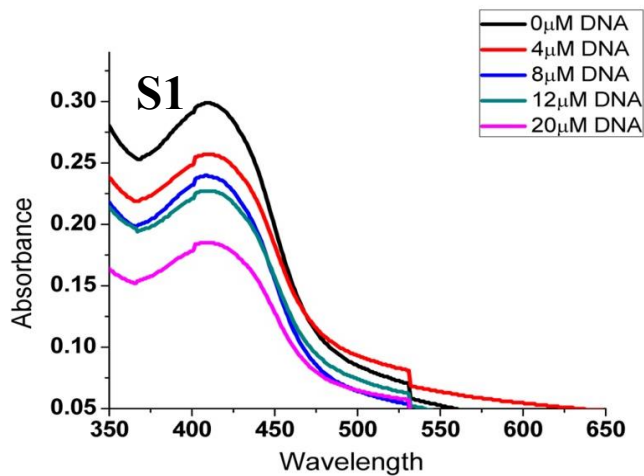
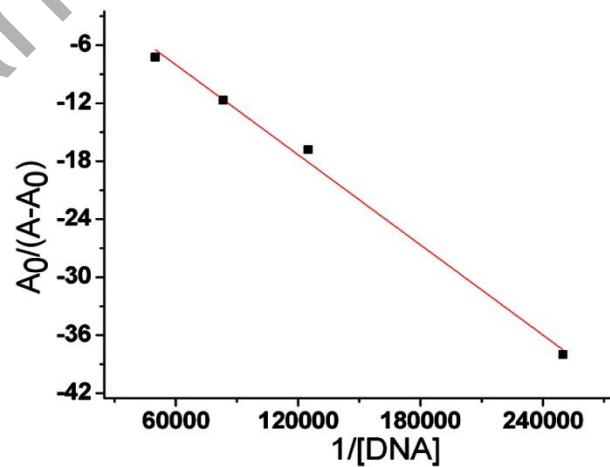
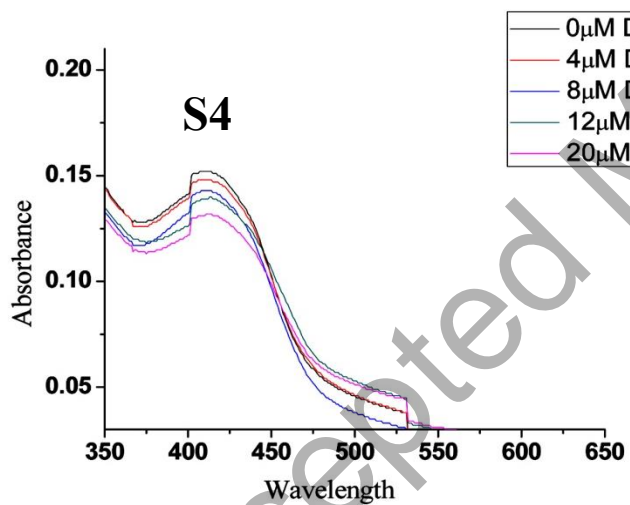
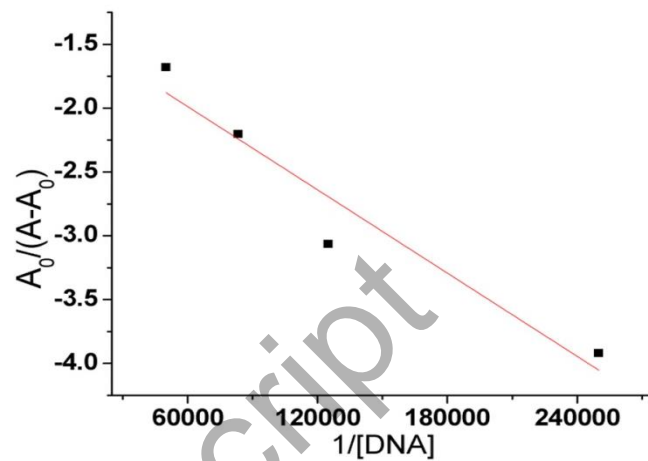
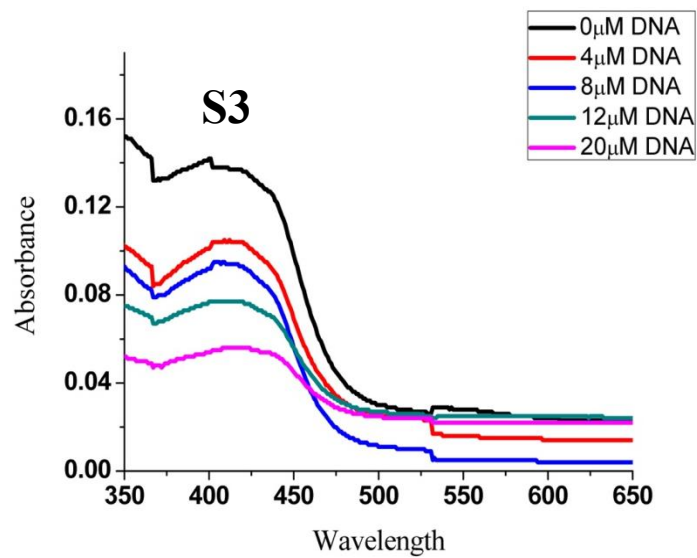


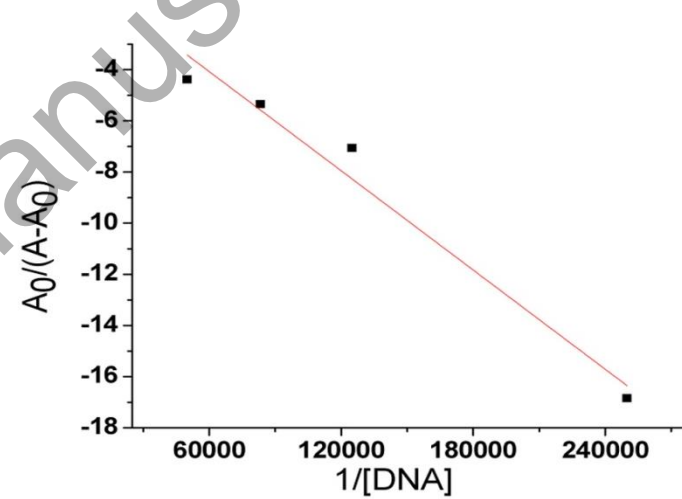
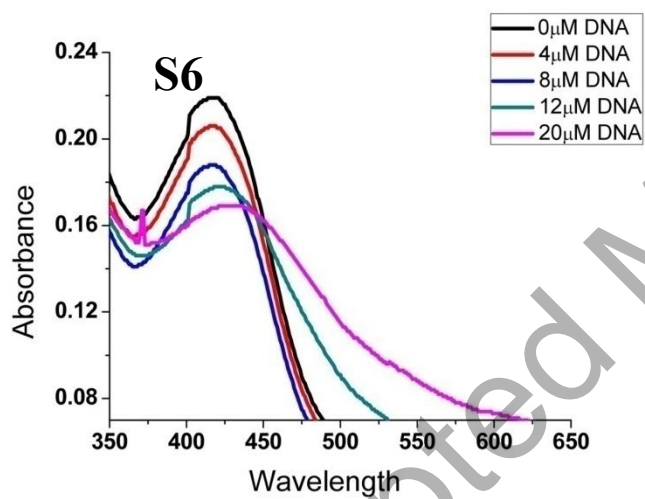
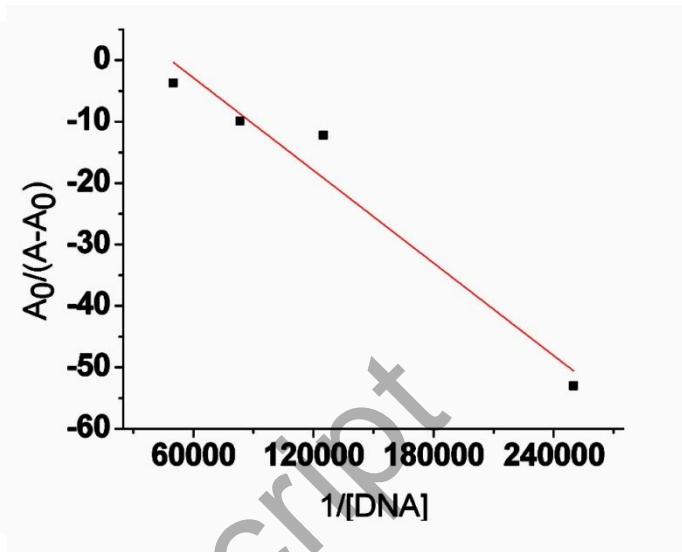
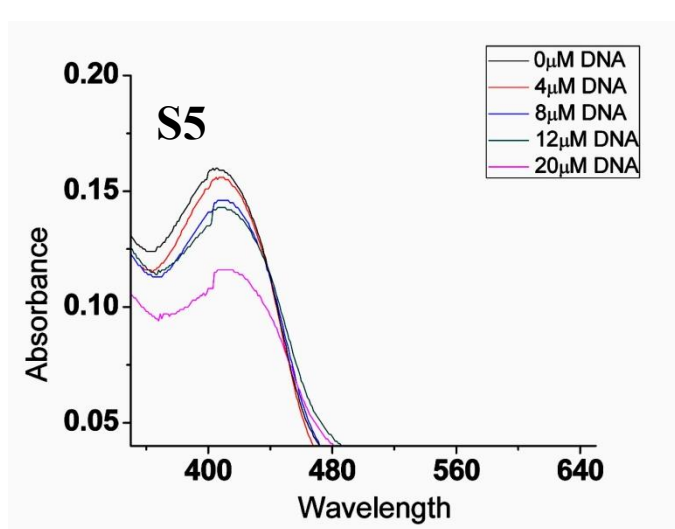
Fig. 2. Cell-cycle analysis of S3 and S4 compounds on HeLa cancer cell line.

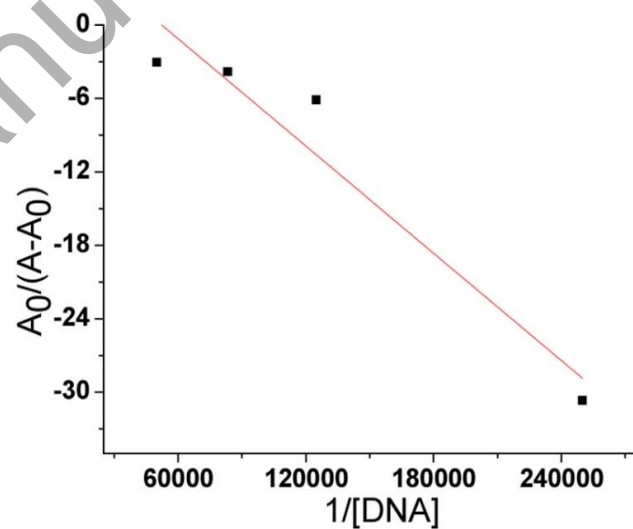
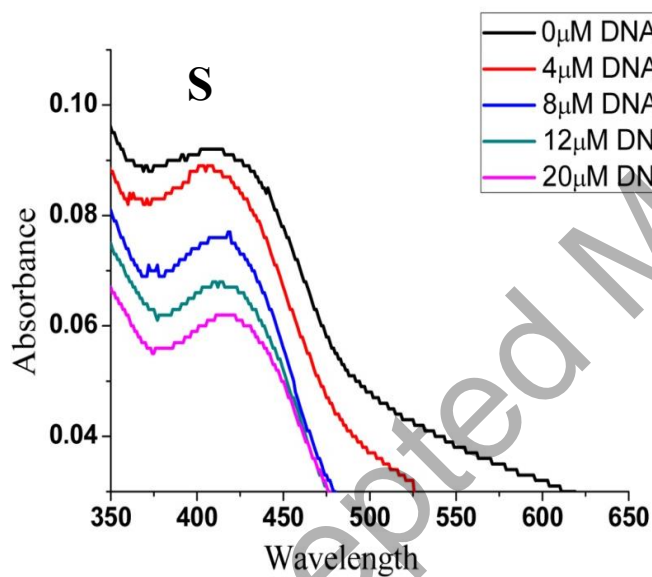
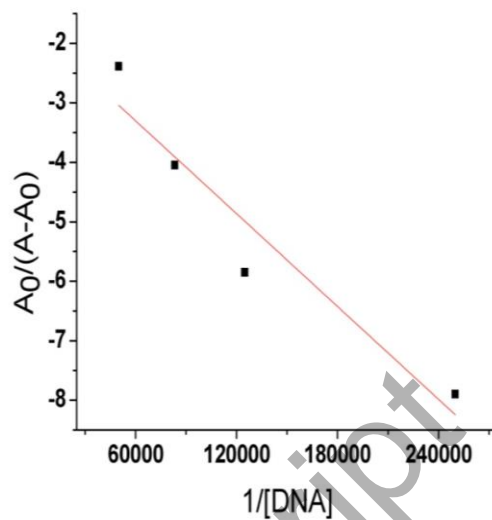
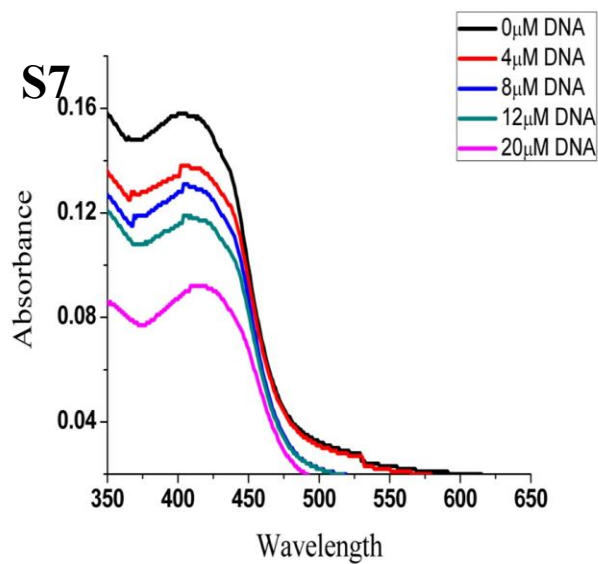
Accepted Manuscript



Accepted Manuscript







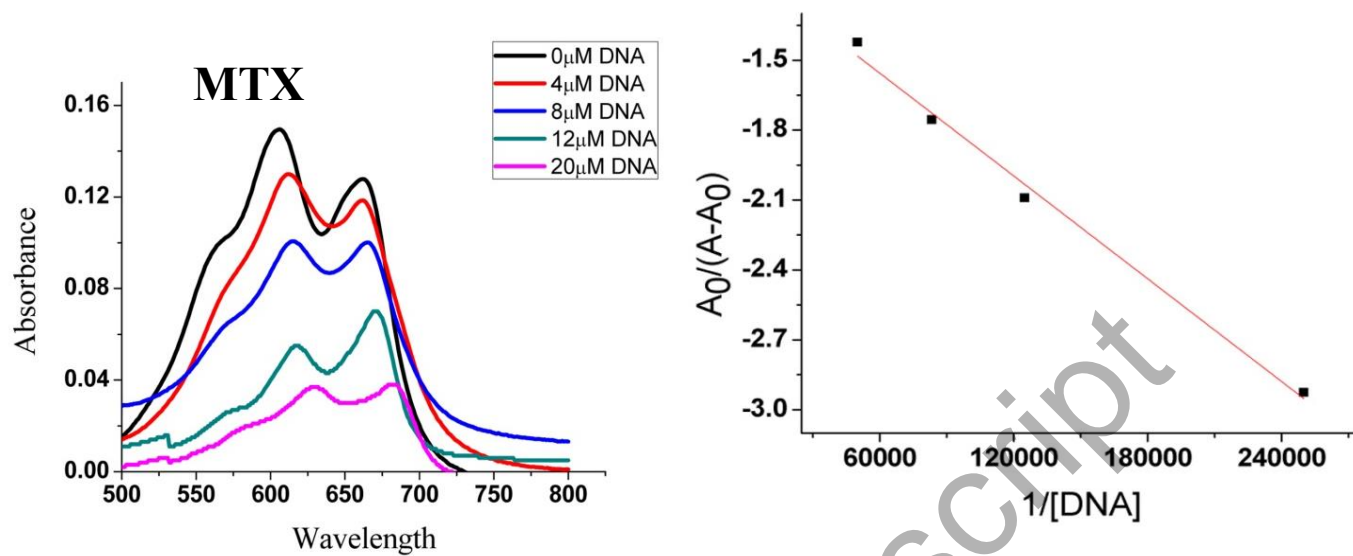
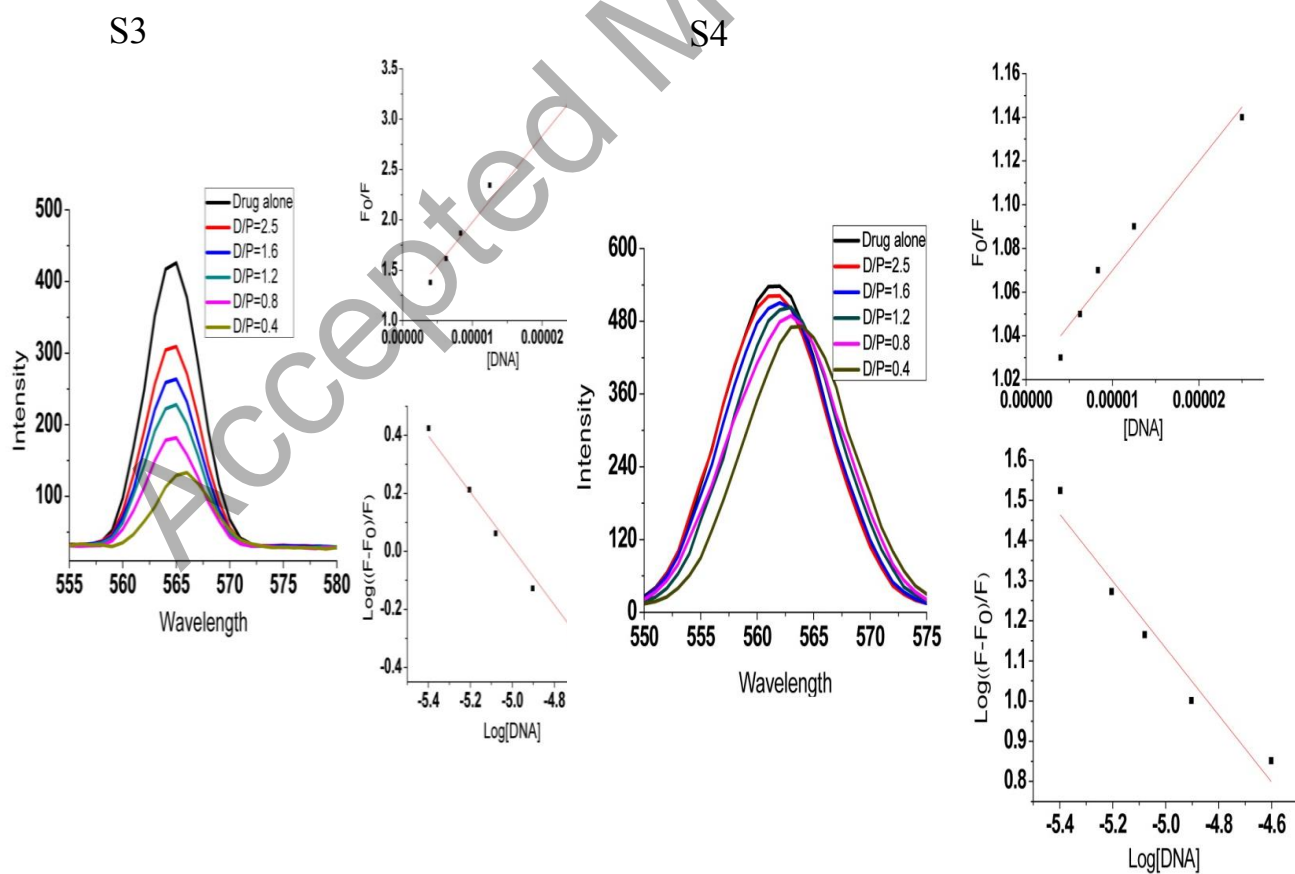
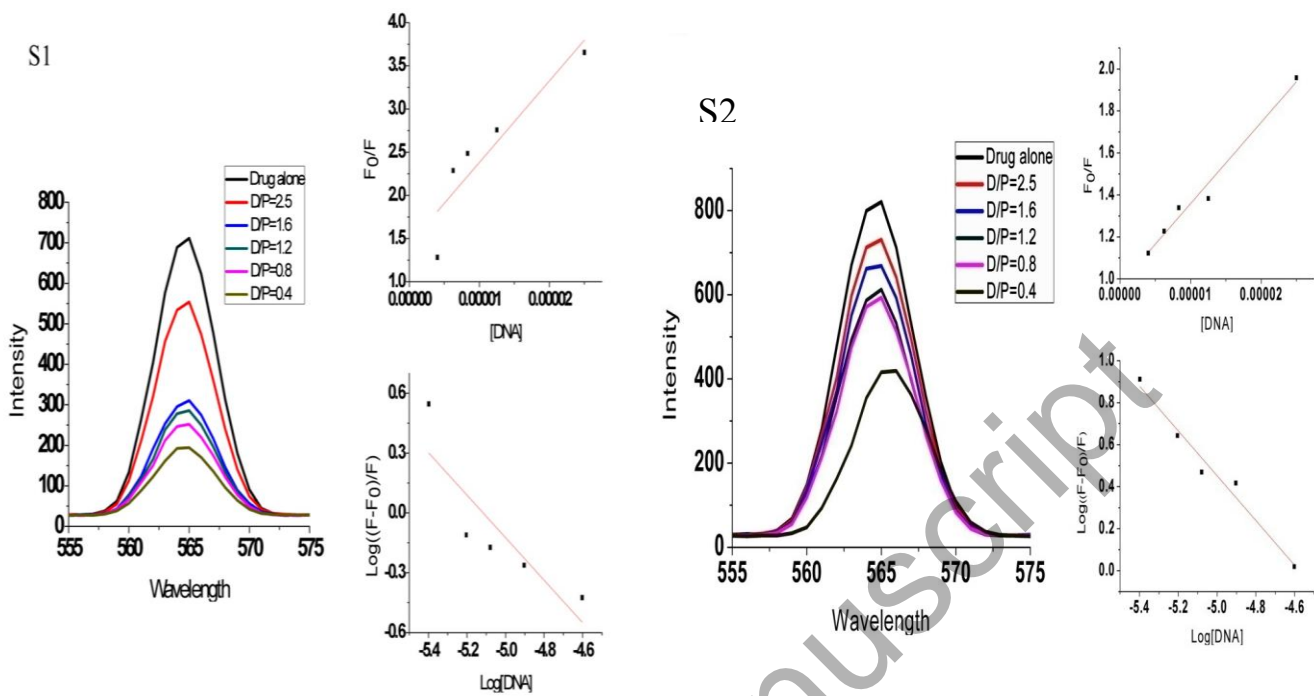
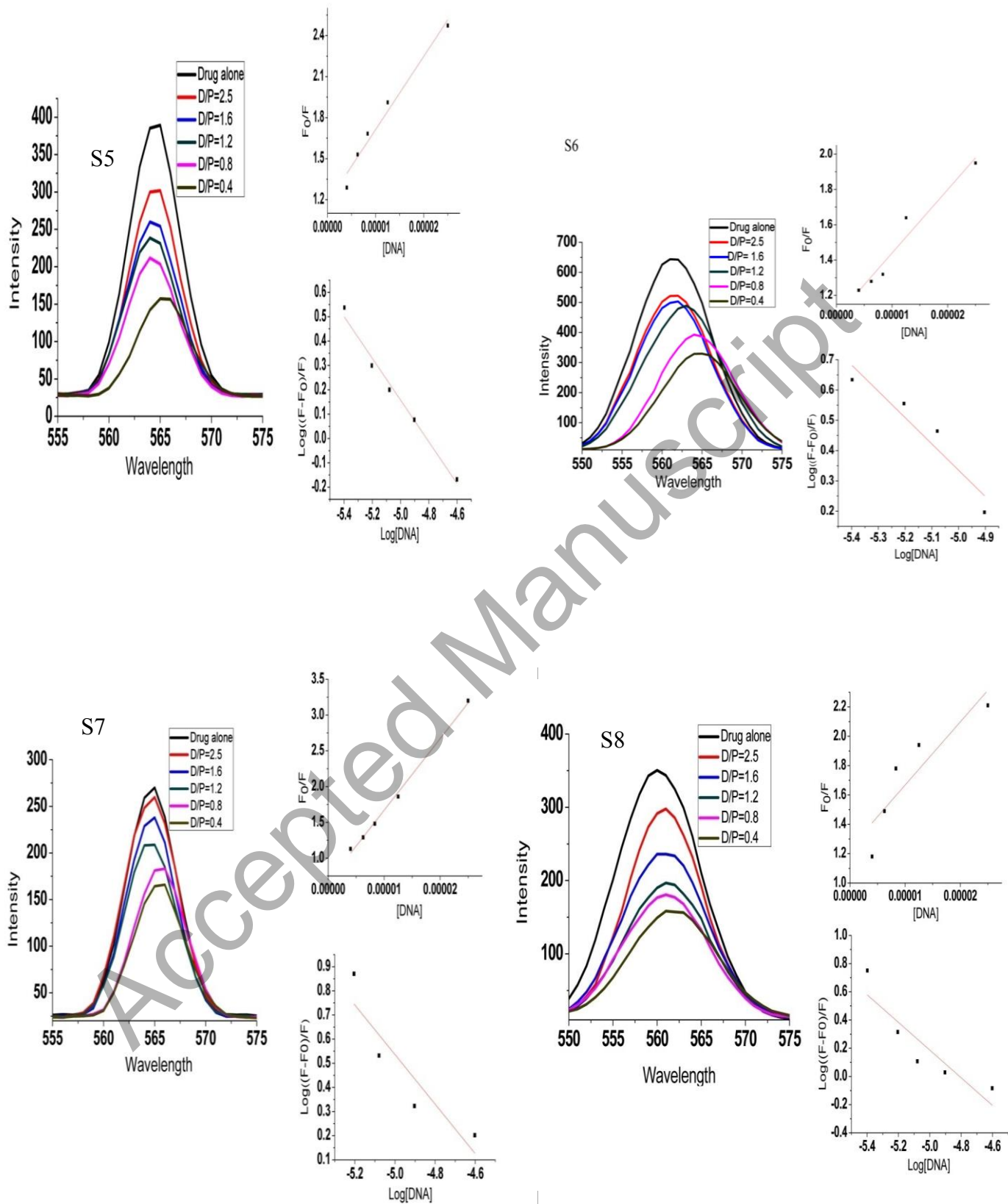


Fig 3. Absorption spectra of 10 μ M of S1, S2, S3, S4, S5, S6, S7, S8 and MTX in absence and presence of ct-DNA at D/P ratios of 2.5, 1.25, 0.83 and 0.5.

Accepted Manuscript





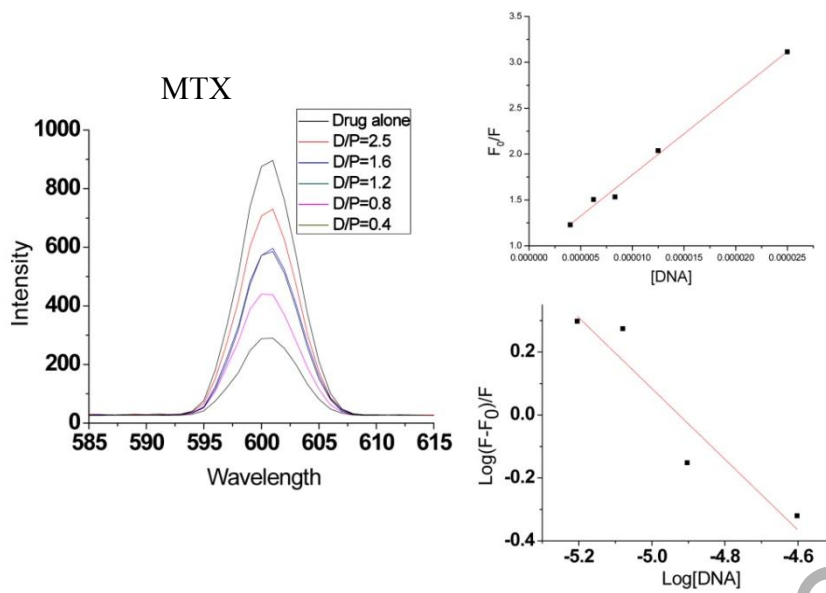


Fig 4. Fluorescence spectra of S1, S2, S3, S4, S5, S6, S7, S8 and MTX (10 μM) drug in phosphate buffer solution (pH=7.1) were recorded with $\lambda_{\text{exc}}=390\text{nm}$ and $\lambda_{\text{em}}=560\text{-}565\text{ nm}$ shift in absence and presence of DNA at D/P ratios of 2.5, 1.6, 1.2, 0.8 and 0.4.

Accepted Manuscript

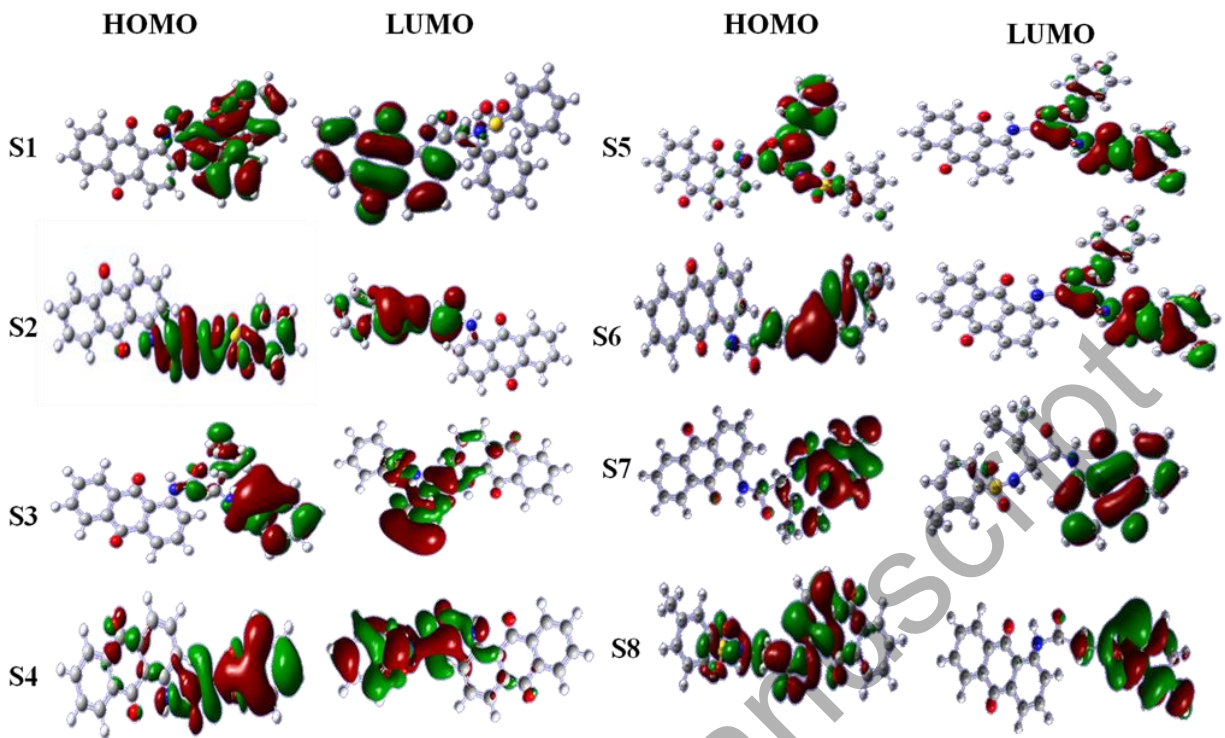


Fig. 5. HOMO-LUMO of the synthesized compounds (S1-S8) were optimized with DFT/B3LYP/ (6-31G (d, p)).

Accepted Manuscript

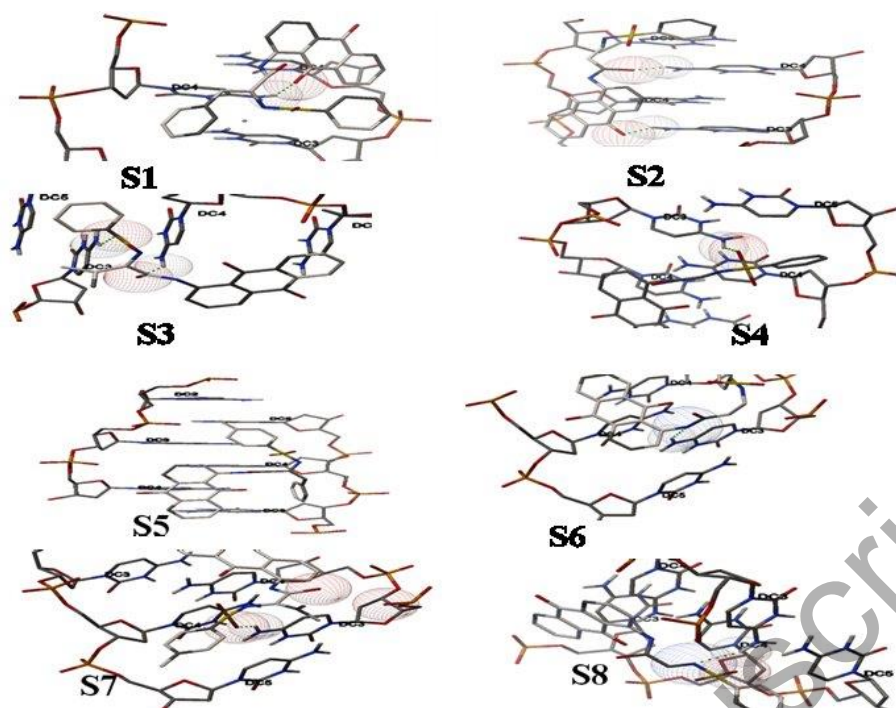


Fig. 6. Schematic representation of H-bond interactions between the sequence d(TCCCC) intermolecular i-motif and synthesized compounds (a) S1 (b) S2 (c) S3 (d) S4 (e) S5 (f) S6 (g) S7 (h) S8.

Accepted Manuscript